# Ynthesis and Characterization of Nonstructural $MG_2NI$ with Replacement Diffusion Method

Yanqiu Jin, Xiuyun Yang, Yunhui Li & Wenjuan Zhang
School of Chemistry and Environmental Engineering
Changchun University of Science and Technology, Changchun 130022, China
E-mail: liyh@cust.edu.cn

Limin Wang & Yaoming Wu
State Key Laboratory of Rare Earth Resource Utilization
Changchun Institute of Applied Chemistry, CAS, Changchun, 130022, China

**Abstract**

Nonstructural $Mg_2Ni$ powder was prepared by replacement-diffusion method. The structure of the $Mg_2Ni$ powder was investigated by X-ray diffraction and transmission electron microscopy. Crystallographic structure analysis showed that the synthesized sample powder was constituted with $Mg_2Ni$ and a small fraction of MgO. The TEM image in low-resolution indicated that the diameter of the synthesized $Mg_2Ni$ powder was in the range of 20~80 nm, and the high-resolution transmission electron microscope (HRTEM) image suggested that the interlinear spacing of (113) lattice planes was 0.229 nm, and the specific surface area examined was 50 $m^2/g$. The electrochemical hydrogen storage capacity of the $Mg_2Ni$ power was also measured in this work. It was 82.5 mAh $g^{-1}$. The reasons of the low capacity hydrogen storage and decrepitating were analyzed, and the mainly cause were the grievous oxidation of the powder and the pulverization.

**Keywords:** $Mg_2Ni$, Replacement-diffusion method, Nanostructure, Characterization

## 1. Introduction

In recently years, many researchers are increasingly interested in researching magnesium and Mg-based Materials for hydrogen storage (Ebrahimi-Purkani,2008,p.211) .(Gennari,2008,p.425) (Gasiorowski,2008,p.283)Because magnesium and Mg-based materials are considered as prospective candidates for hydrogen storage owing to high theoretic hydrogen storage capacity, light weight and low cost. $Mg_2Ni$ intermetallic compound can store hydrogen 3.6 mass % in theory (Reilly, 1968, p.2254). However, it is difficult to obtain $Mg_2Ni$ by conventional melting method because of the large differences in vapor pressure and melting point between Mg and Ni. Furthermore, it is difficult to avoid oxidation of magnesium during the preparation, for example, using mechanical alloying (Zaluski,1995,p.70), bulk mechanical alloying(Aizawa,1999,p.248), vapor phase process (Ueda,2005,p.253), combustion synthesis method (Kodera,2007,p.138), etc. These are also one of aspects resulted in $Mg_2Ni$ has not widely applications, besides high working temperature and poor dynamics of desorption hydrogen. The nanostructure of $Mg_2Ni$ can improve the properties. In some aspects, the nonstructural $Mg_2Ni$ power possesses superior properties such as larger specific surface area, which is beneficial to improving the dynamics of $Mg_2Ni$ desorption hydrogen. More and more researchers are preparing Mg-based materials with nanostructure by ball milling method at the present time(Inoue,1998,p.2221)(Inoue,1999,p.312)(Cui,1999,p.3549). It is known that it is more difficult to prepare nonstructural $Mg_2Ni$ intermetallic compounds power by conventional melting method except for ball milling method. Huatang Yuan et al. have prepared the powder $Mg_2Cu$( Panwen,1982,p.580), $Mg_2Ni$ (Panwen,1986,p.831), $Mg_2Ni_{0.75}Cu_{0.25}$ (Zhang,1990,p.1431), $Mg_2Ni_{0.75}Pd_{0.25}$ (Zhang,1990,p.1431) by replacement-diffusion method (RDM), and analyzed desorption hydrogen temperature of the hydride of $Mg_2Ni$ in the process of charge/discharge hydrogen measurement. In present work, nonstructural $Mg_2Ni$ powder is prepared by RDM, and the structure and electrochemical hydrogen storage capacity of the powder are investigated.

## 2. Experimental Procedure

The nonstructural $Mg_2Ni$ powder was synthesized by replacement-diffusion method. Both Mg powder (purity of 99.8%) and anhydrous $NiCl_2$ were weighed the correct proportion and reacted in dry dimethyl-formamide (DMF) in a 250ml flask. The mixture was stirred for homogeneity, and the temperature of the reaction was kept at 323K ~ 333K for 3h. The precipitate of Mg and Ni (sample B) was filtered and washed with dry acetone. Then the

precipitate was heated protected under an argon atmosphere in a tubular resistor furnace. The products were heated to 823K and held at this temperature for 3h. After cooling to ambient, the products were dark grey powder (sample C). The phase structure of the synthesized powder was determined by X-ray diffraction (XRD) analysis. The XRD analysis was performed using a Rigaku D/max 2500 PC X-ray diffract meter with Cu (Kα) radiation. The nature of the surface of the synthesized powder was observed by high-resolution transmission electron microscope(HRTEM,JEM-2100HR).the Brunauer-Emment-Teller(BET)nitrogen adsorption-desorption was measured, which is a Nova-1000 Surface Area Analyzer. A three-electrode system was used for charging/discharging tests on automatic Galvan static charge-discharge apparatus (DC-5), where the sample disc acted as the negative electrode, sintered $Ni(OH)_2$/NiOOH the counter electrode and a Hg/HgO reference electrode in the 6M KOH electrolyte at ambient. For each charge/discharge cycle, the electrodes were charged at 60 mA /g for 2h, rested for 10min, and then discharged at 20 mA /g to a cut off voltage of 0.6 V.

## 3. Results and discussion

Fig. 1 shows XRD patterns for $Mg_2Ni$ power during different preparation sections. Fig. 1 presents the XRD of the synthesized $Mg_2Ni$ alloy powder: sample A, pure Nickel power; sample B, before heated and sample C heated at 823K for 3h. It can be obviously from sample A and B; three diffraction peaks of pure Nickel power (sample A) gradually become broader with the proceeding of replacement reaction, suggesting the formation of nanostructure Ni (sample B). The peaks intensity for magnesium becomes weaker. It is indicated that Nan crystalline $Mg_2Ni$ alloy power is formed by heated in argon atmosphere at 823K for 3h. Peaks for MgO are also observed in C sample because of oxidation of magnesium during the heat-treated process.

Fig. 2 is the TEM image in low-resolution of the $Mg_2Ni$ powder. Fig. 2 clearly reveals that the morphology of the $Mg_2Ni$ power is the approximate spherical particle, the diameter of the particle is in the range of 20~80 nm. The HRTEM image of the power is shown in Fig. 3. It can be observed from the HRTEM image that an interlinear spacing is 0.229 nm. We can arrival conclusions that lattice planes corresponding with the interlinear spacing is (113) lattice planes of $Mg_2Ni$. And the interlinear separation angle between (113) and (113) is 59.41°, the measured result is approximately equal to the theory calculated value. As a result, the sample C is assigned to the hexagonal crystal structure of $Mg_2Ni$ with cell parameters of a = 5.216 Å and c = 13.23 Å. The structure is a hexagonal symmetry and belongs to space group $P6_222$ (Schefer, 1980, p.65).

The discharging behavior of the synthesized $Mg_2Ni$ powder is shown in Fig. 4. The discharge current density is 20 mA/g at room temperature. It is indicated from Fig. 4 that the maximum discharge capacity of $Mg_2Ni$ is attained at the second cycle. It suggests that the $Mg_2Ni$ is hardly needed to active. The electrochemical capacity of $Mg_2Ni$ is 82.5 mAh/g. The capacity has been improved compared with 10 mA /g capacity of $Mg_2Ni$ prepared by N. Cui et al. (Luan, 1996, p.373). To analyze the result we take into account that the nanostructure of $Mg_2Ni$ has a large number of defects on the surface. It results in more transfer reaction active for absorption /desorption of hydrogen, and brought forward to improve discharge capacity. The electrochemical capacity of the $Mg_2Ni$ powder decreases gradually. It is mainly because Mg, which is on the surface of the $Mg_2Ni$, is gradually corroded in the alkaline electrolyte. And it can slowly form an oxide layer, which will have a negative effect on hydrogen diffusion and the charge transfer reaction on the surface of the powder. However, after several hydriding /dehydriding cycles, the electrochemical capacity augments again. It is induced by the crystal lattice of the powder expanding, the oxide layer falling into pieces, and engendering a novel surface. This process can be observed clearly in the Fig. 4. The properties of the $Mg_{2-x}Al_xNi\{x= [0, 0.5]\}$ reported by Yuan et al. (Yuan, 2000, p.208) is similar to he result of in the present work.

The specific surface area of the $Mg_2Ni$ power is 50 $m^2/g$ examined by the BET technique using nitrogen in the micrometric analyzer. Z. Debouche et al. (Dehouche, 1999, p.312) have reported the specific surface area of Nan crystalline $Mg_2Ni$ alloy power prepared by high energy ball milling is 10.97 $m^2/g$, and has not produced significant decrepitating during the dynamic hydrogen absorption/desorption cycles. Our result suggests the specific area has an effect on decrepitating of the hydrogen storage capacity of $Mg_2Ni$. The effect results are indistinct, and need further investigate.

Figure. 5 show the electrochemical impedance spectra of $Mg_2Ni$. As can be seen from the figure, the shape of $Mg_2Ni$ alloy electrode impedance curves are two semi-circles, indicating that in the process of hydrogen absorption and desorption process, the electrochemical polarization and concentration polarization exist the same time.

Alternating current impedance test results show that the series alloy electrode reaction rate-controlling step is controlled by the charge transfer between the alloy / electrolyte interface.

**Acknowledgments**

This work is financially supported by CAS for Distinguished Talents Program. The authors would like to express their thanks to Dr. Chunfei Li working in Portland State University, USA for beneficial explanation for the HRTEM image.

**References**

Aizawa, T., Kuji, T. & Nakano, H. (1999). Synthesis of $Mg_2Ni$ alloy by bulk mechanical alloying. *J. Alloys Compd.* 291. 248-253.

Cui, N., He, P. & Luo, J. L. (1999). Synthesis and characterization of Nan crystalline magnesium-based hydrogen storage alloy electrode materials. *Electro him. Acta*. 44, 3549-3558.

Debouche, Z, Djaozandry, R., Goyette, J. & Bose, T. K. (1999). Thermal cyclic charge and discharge stability of Nan crystalline $Mg_2Ni$ alloy. *J. Alloys Compd*. 288.312-318.

Debouche, Z., Djaozandry, R., Goyette, J. & Bose, T. K. (1999). Thermal cyclic charge and discharge stability of Nan crystalline $Mg_2Ni$ alloy. *J. Alloys Compd*. 288, 312-318.

Ebrahimi-Purkani, A. &Kashani-Bozorg, S. F. (2008). Nan crystalline $Mg_2Ni$-based powders produced by high-energy ball milling and subsequent annealing. *J. Alloys Compd... 456.* 211-215.

Gasiorowski A., Iwasieczko W., Skoryna, D., Drulis, H. & Jurczyk, M. (2004). Hydriding properties of nanocrystalline $Mg_{2-x}M_xNi$ alloys synthesized by mechanical alloying (M=Mn, Al). *J. Alloys Compd*. 364.283-288.

Gennari, F. C. & Esquivel M. R. (2008). Structural characterization and hydrogen sorption properties of Nan crystalline $Mg_2Ni$. *J. Alloys Compd.* 459. 425-432.

Inoue, H., Hazui, S., Nohara, S. &Iwakura, C. (1998).Preparation and electrochemical characterization of $Mg_2Ni$ alloys with different crystallinities . *Electro him. Acta.* 43, 2221-2224.

Kodera,Y.,Yamasaki,N.,Yamamoto,T.,Kawasaki,T.,Ohyanagi,M.&Munir,Z.A. (2007). Hydrogen storage $Mg_2Ni$ alloy produced by introduction field activated combustion synthesis. *J. Alloys Compd.* 446-447. 138-141.

Luan, B., Cui, N., Zhao, H. J., Lin, H. K. & Dou, S. X. (1996). Effects of potassium-boron addition on the performance of titanium based hydrogen storage alloy electrodes. *J. Alloys Compd. 21*.373-379.

Panwen, S., Yunshi, Z., Huatang, Y. & Shengchang, C. (1982). A new method for the synthesis of hydrogen storage compounds – replacement-diffusion method for $Mg_2Cu$. *Chem. J. Chin. Uni.* 3, 580-582.

Panwen, S., Yunshi, Z., Song, Z., Xiandao, F. ,Huatang, Y. & Shengchang, C. (1986). Chemical synthesis of hydrogen-storing alloys (III) Replacement-diffusion method for $Mg_2Ni_{0.75}Cu_{0.25}$, *Hydrogen Energy Progress **VI**,* 831–837.

Reilly, J. J. & Wiswall, R. H. (1968). The Reaction of Hydrogen with Alloys Magnesium and nickel and the Formation of $Mg_2NiH_4$.*J. Inorg. Chem*. 7. 2254.

Schafer, J. , Fischer, P. & Halg, W. (1980). New structure results for hydrides and deuterides of the hydrogen storage material $Mg_2Ni$. *J. Less-Common Metals*.74, 65-73.

Ueda, T. T., Tsukahara, M., Kamiya, Y. & Kikuchi, S. (2005). Preparation and hydrogen storage properties of Mg–Ni–$Mg_2Ni$ laminate composites. *Alloys Compd*. 386.253-257.

Yuan, H. T., Wang, L. B. , Cao, R. , Wang, Y. J. , Zhang, Y. S. , Yan, D. Y. , Zhang, W. H. & Gong, W.L. (2000). Electrochemical characteristics of $Mg_{2-x}Al_xNi$ ($0 \le x \le 0.5$). *J.Alloys Compd.* 309.208-211.

Zaluski, L. , Zaluska, A. & Ström-Olsen, J. O. (1995) . Nan crystalline metal hydrides. *J. Alloys Compd.* 253-254. 70-79.

Zhang, Y. S. , Ji, J. H., Yuan, H. T. , Chen, S. C. & Wang, D. (1990).Synthesis of ternary alloys $Mg_2Ni_{0.75}Pd_{0.25}$ and studies on its surface properties. *J. Mater. Res.* 5, 1431-1434.

Zhang, Y. S., Ji, J.H., Yuan,H.T., Chen,sS.C., Wang,D.& Zhang,T.S. (1990). Synthesis of ternary alloys $Mg_2Ni_{0.75}Pd_{0.25}$ and studies on its surface properties. *J. Mater.Res.* 5.1431-1434.

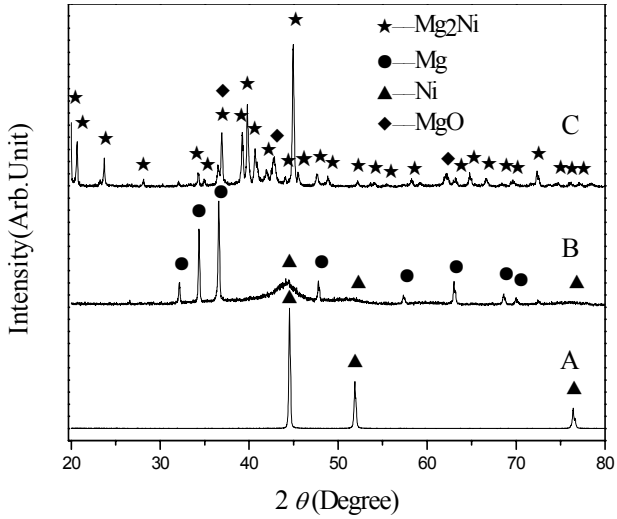


Figure 1. XRD pattern of the synthesized $Mg_2Ni$ powder by RDM: pure Nickel (A); before heated (B) and after heated (C).

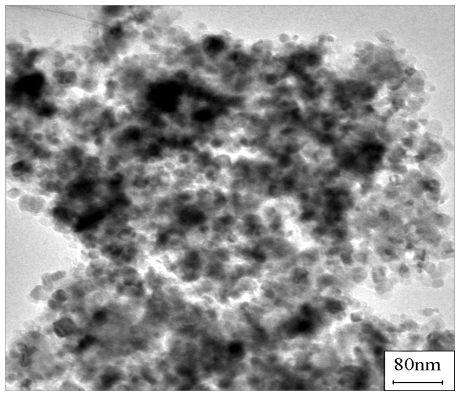


Figure 2. The TEM image of the synthesized $Mg_2Ni$ powder

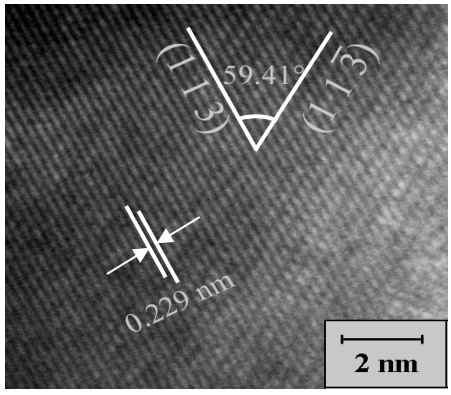


Figure 3. The HRTEM image of the synthesized $Mg_2Ni$ powder

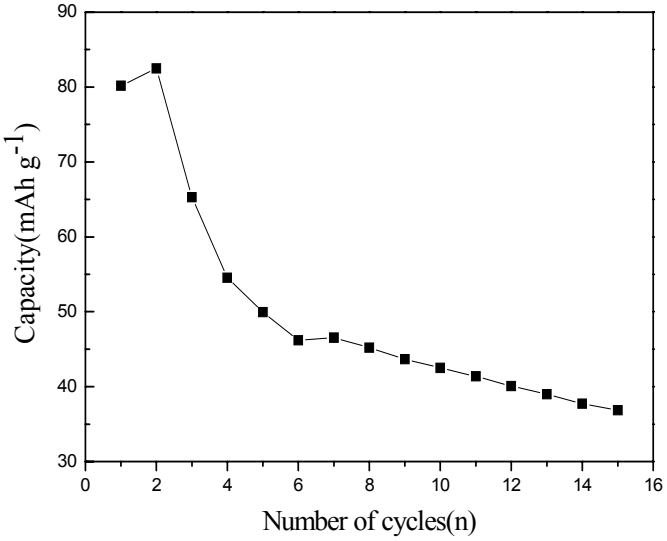


Figure 4. Discharge capacity curve of $Mg_2Ni$ prepared by RDM

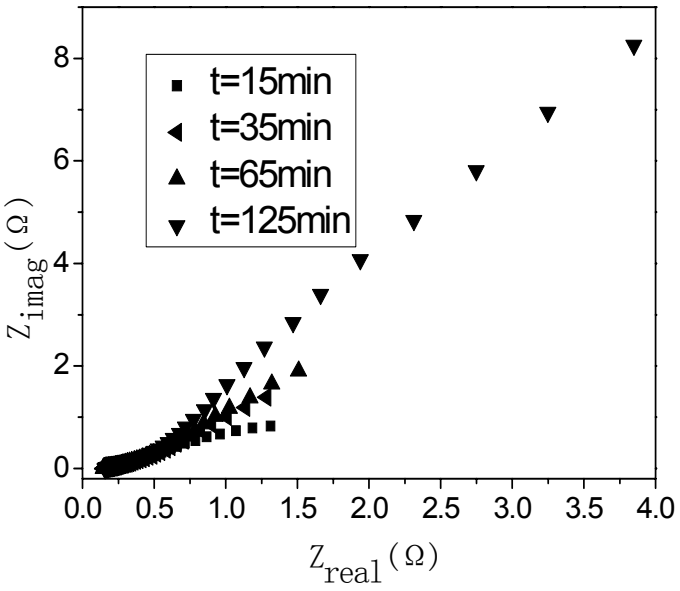


Figure 5. Electrochemical impedance spectra of $Mg_2Ni$ electrodes at different discharge depths


ISSN 1913-1844 E-ISSN 1913-1852

# Prime Cordial Labeling for Some Graphs

S K Vaidya (Corresponding author)
Department of Mathematics, Saurashtra University
Rajkot 360 005, Gujarat, India
E-mail: samirkvaidya@yahoo.co.in

P L Vihol
Mathematics Department, Government Polytechnic
Rajkot 360 003, Gujarat, India
E-mail: viholprakash@yahoo.com

**Abstract**

We present here prime cordial labeling for the graphs obtained by some graph operations on given graphs.

**Keywords:** Prime cordial labeling, Total graph, Vertex switching

## 1. Introduction

We begin with simple, finite, connected and undirected graph $G = (V(G),E(G))$. For all standard terminology and notations we follow (Harary F., 1972). We will give brief summary of definitions which are useful for the present investigations.

*Definition 1.1* If the vertices of the graph are assigned values subject to certain conditions then it is known as *graph labeling*.

For a dynamic survey on graph labeling we refer to (Gallian J., 2009). A detailed study on variety of applications of graph labeling is reported in (Bloom G. S., 1977, p. 562-570).

*Definition 1.2* Let $G$ be a graph. A mapping $f: V(G) \rightarrow \{0, 1\}$ is called *binary vertex labeling* of $G$ and $f(v)$ is called the label of the vertex $v$ of $G$ under $f$.

For an edge $e = uv$, the induced edge labeling $f^*: E(G) \rightarrow \{0, 1\}$ is given by $f^*(e) = |f(u) - f(v)|$. Let $v_f(0)$, $v_f(1)$ be the number of vertices of $G$ having labels $0$ and $1$ respectively under $f$ while $e_f(0)$, $e_f(1)$ be the number of edges having labels $0$ and $1$ respectively under $f^*$.

*Definition 1.3* A binary vertex labeling of a graph $G$ is called a *cordial labeling* if $|v_f(0) - v_f(1)| \leq 1$ and $|e_f(0) - e_f(1)| \leq 1$. A graph $G$ is *cordial* if it admits cordial labeling.

The concept of cordial labeling was introduced by (Cahit I.,1987, p.201-207). After this many researchers have investigated graph families or graphs which admit cordial labeling. Some labeling schemes are also introduced with minor variations in cordial theme. Some of them are product cordial labeling, total product cordial labeling and prime cordial labeling. The present work is focused on prime cordial labeling.

*Definition 1.4 A prime cordial labeling* of a graph $G$ with vertex set $V(G)$ is a bijection $f : V(G) \rightarrow \{1,2,3,.....|V(G)|\}$ defined by $f(e = uv) = 1$ ; if $gcd(f(u), f(v)) = 1$

$= 0$ ; *otherwise*

and $|e_f(0) - e_f(1)| \leq 1$. A graph which admits prime cordial labeling is called a prime cordial graph.

*Definition 1.5* Let $G$ be a graph with two or more vertices then the *total graph* $T(G)$ of a graph $G$ is the graph whose vertex set is $V(G) \cup E(G)$ and two vertices are adjacent whenever they are either adjacent or incident in $G$.

*Definition 1.6* The *composition* of two graphs $G_1$ and $G_2$ denoted by $G_1[G_2]$ has vertex set $V(G_1[G_2]) = V(G_1) \times V(G_2)$ and edge set $E(G_1[G_2]) = \{(u_1,v_1)(u_2,v_2) / \; u_1u_2 \in E(G_1)$ or $[u_1 = u_2$ and $v_1v_2 \in E(G_2)]\}$

*Definition 1.7 A vertex switching* $G_v$ of a graph $G$ is the graph obtain by taking a vertex $v$ of $G$, removing all the edges incident to $v$ and adding edges joining $v$ to every other vertex which are not adjacent to $v$ in $G$.

## 2. Main Results

*Theorem 2.1* $T(P_n)$ is prime cordial graph, $\forall\, n \geq 5$.

*Proof* : If $v_1, v_2, v_3, \ldots v_n$ and $e_1, e_2, e_3, \ldots e_n$ be the vertices and edges of $P_n$ then $v_1, v_2, v_3, \ldots v_n, e_1, e_2, e_3, \ldots e_n$ are vertices of $T(P_n)$.

We define vertex labeling $f: V(T(P_n)) \rightarrow \{1, 2, 3 \ldots |V(G)|\}$ as follows. We consider following four cases.

Case 1: $n = 3, 5$

For the graph $T(P_3)$ the possible pairs of labels of adjacent vertices are (1,2), (1,3), (1,4), (1,5), (2,3), (2,4), (2,5), (3,4), (3,5), (4,5). Then obviously $e_f(0) = 1$, $e_f(1) = 6$. That is, $|e_f(0) - e_f(1)| = 5$ and in all other possible arrangement of vertex labels $|e_f(0) - e_f(1)| > 5$. Therefore $T(P_3)$ is not a prime cordial graph.

The case when $n$=5 is to be dealt separately. The graph $T(P_5)$ and its prime cordial labeling is shown in *Fig 1*.

Case 2: $n$ odd, $n \geq 7$

$f(v_1) = 2, f(v_2) = 4,$

$f(v_{i+2}) = 2(i + 3), \quad 1 \leq i \leq \lfloor n/2 \rfloor - 2$

$f(v_{\lfloor n/2 \rfloor + 1}) = 3, f(v_{\lfloor n/2 \rfloor + 2}) = 1, f(v_{\lfloor n/2 \rfloor + 3}) = 7,$

$f(v_{\lfloor n/2 \rfloor + 2 + i}) = 4i + 9, 1 \leq i \leq \lfloor n/2 \rfloor - 2$

$f(e_i) = f(v_{\lfloor n/2 \rfloor}) + 2i, 1 \leq i \leq \lfloor n/2 \rfloor - 1,$

$f(e_{\lfloor n/2 \rfloor}) = 6, f(e_{\lfloor n/2 \rfloor + 1}) = 9, f(e_{\lfloor n/2 \rfloor + 2}) = 5,$

$f(e_{\lfloor n/2 \rfloor + i + 1}) = 4i + 7, 1 \leq i \leq \lfloor n/2 \rfloor - 2$

In this case we have $e_f(0) = e_f(1) + 1 = 2(n-1)$

Case 3: $n = 2, 4, 6$

For the graph $T(P_2)$ the possible pairs of labels of adjacent vertices are (1,2), (1,3), (2,3). Then obviously $e_f(0) = 0$, $e_f(1) = 3$. Therefore $T(P_2)$ is not a prime cordial graph.

For the graph $T(P_4)$ the possible pairs of labels of adjacent vertices are (1,2), (1,3), (1,4), (1,5), (1,6), (1,7), (2,3), (2,4), (2,5), (2,6), (2,7), (3,4), (3,5), (3,6), (3,7), (4,5), (4,6), (4,7), (5,6), (5,7), (6,7). Then obviously $e_f(0) = 4$, $e_f(1) = 7$. That is, $|e_f(0) - e_f(1)| = 3$ and in all other possible arrangement of vertex labels $|e_f(0) - e_f(1)| > 3$. Thus $T(P_4)$ is not a prime cordial graph.

The case when $n$=6 is to be dealt separately. The graph $T(P_6)$ and its prime cordial labeling is shown in *Fig 2*.

Case 4 n even, $n \geq 8$

$f(v_1) = 2, f(v_2) = 4,$

$f(v_{i+2}) = 2(i + 3), \quad 1 \leq i \leq n/2 - 3$

$f(v_{n/2}) = 6, f(v_{n/2+1}) = 9, f(v_{n/2+2}) = 5,$

$f(v_{n/2+2+i}) = 4i + 7, 1 \leq i \leq n/2 - 2$

$f(e_i) = f(v_{n/2-1}) + 2i, 1 \leq i \leq n/2 - 1,$

$f(e_{n/2}) = 3, f(e_{n/2+1}) = 1, f(e_{n/2+2}) = 7,$

$f(e_{n/2+2+i}) = 4i + 9, 1 \leq i \leq n/2 - 3$

In this case we have $e_f(0) = e_f(1) + 1 = 2(n-1)$

That is, $T(P_n)$ is a prime cordial graph, $\forall\, n \geq 5$.

*Illustration 2.2* Consider the graph $T(P_7)$. The labeling is as shown in *Fig 3*.

*Theorem 2.3* $T(C_n)$ is prime cordial graph, $\forall\, n \geq 5$.

*Proof* : If $v_1, v_2, v_3, \ldots v_n$ and $e_1, e_2, e_3, \ldots e_n$ be the vertices and edges of $C_n$ then $v_1, v_2, v_3, \ldots v_n, e_1, e_2, e_3, \ldots e_n$ are vertices of $T(C_n)$.

We define vertex labeling $f: V(T(C_n)) \rightarrow \{1, 2,3, \ldots |V(G)|\}$ as follows. We consider following four cases.

Case 1: $n = 4$

For the graph $T(C_4)$ the possible pair of labels of adjacent vertices are (1,2), (1,3), (1,4), (1,5), (1,6), (1,7), (1,8), (2,3), (2,4), (2,5), (2,6), (2,7), (2,8), (3,4), (3,5), (3,6), (3,7), (3,8), (4,5), (4,6), (4,7), (4,8), (5,6), (5,7), (5,8), (6,7), (6,8), (7,8) . Then obviously $e_f(0) = 6$, $e_f(1) = 10$. That is, $|e_f(0) - e_f(1)| = 4$ and all other possible arrangement of vertex labels will yield $|e_f(0) - e_f(1)| > 4$. Thus $T(C_4)$ is not a prime cordial graph.

*Case 2: n even, n ≥ 6*

$f(v_1) = 2, f(v_2) = 8,$

$f(v_{i+2}) = 4i + 10, \quad 1 \leq i \leq n/2 - 3$

$f(v_{n/2}) = 12, f(v_{n/2+1}) = 3, f(v_{n/2+2}) = 9, f(v_{n/2+3}) = 7,$

$f(v_{n/2+2+i}) = 4i + 9, 1 \leq i \leq n/2 - 3$

$f(e_1) = 4, f(e_2) = 10,$

$f(e_{i+2}) = 4(i + 3), 1 \leq i \leq n/2 - 3,$

$f(e_{n/2}) = 6, f(e_{n/2+1}) = 1, f(e_{n/2+2}) = 5,$

$f(e_{n/2+1+i}) = 4i + 7, 1 \leq i \leq n/2 - 2$

In view of the labeling pattern defined above we have

$e_f(0) = e_f(1) = 2n.$

*Case 3: n = 3*

For the graph $T(C_3)$ the possible pairs of labels of adjacent vertices are (1,2), (1,3), (1,4), (1,5), (1,6), (2,3), (2,4), (2,5), (2,6), (3,4), (3,5), (3,6), (4,5), (4,6), (5,6). Then obviously $e_f(0) = 4$, $e_f(1) = 8$. That is, $|e_f(0) - e_f(1)| = 4$ and all other possible arrangement of vertex labels will yield $|e_f(0) - e_f(1)| > 4$. Thus $T(C_3)$ is not a prime cordial graph.

*Case 4: n odd, n ≥ 5*

$f(v_1) = 2,$

$f(v_{1+i}) = 4(i + 1), \quad 1 \leq i \leq \lfloor n/2 \rfloor - 1$

$f(v_{\lfloor n/2 \rfloor+1}) = 6, f(v_{\lfloor n/2 \rfloor+2}) = 9, f(v_{\lfloor n/2 \rfloor+3}) = 5,$

$f(v_{\lfloor n/2 \rfloor+3+i}) = 4i + 7, 1 \leq i \leq n - \lfloor n/2 \rfloor - 3$

$f(e_1) = 4,$

$f(e_{1+i}) = 4i + 6, 1 \leq i \leq \lfloor n/2 \rfloor - 1,$

$f(e_{\lfloor n/2 \rfloor+1}) = 3, f(e_{\lfloor n/2 \rfloor+2}) = 1, f(e_{\lfloor n/2 \rfloor+3}) = 7,$

$f(e_{\lfloor n/2 \rfloor+3+i}) = 4i+9, 1 \leq i \leq n - \lfloor n/2 \rfloor - 3$

In view of the labeling pattern defined above we have

$e_f(0) = e_f(1) = 2n.$

Thus $f$ is a prime cordial labeling of $T(C_n)$.

*Illustration 2.4* Consider the graph $T(C_6)$. The labeling is as shown in *Fig 4*.

*Theorem 2.5* $P_2 [P_m]$ is prime cordial graph $\forall$ m ≥ 5.

*Proof* : Let $u_1, u_2, u_3, \ldots, u_m$ be the vertices of $P_m$ and $v_1, v_2$ be the vertices of $P_2$. We define vertex labeling $f: V(P_2 [P_m]) \rightarrow \{1, 2, 3, \ldots, |V(G)|\}$ as follows. We consider following four cases.

*Case 1: m = 2, 4*

For the graph $P_2 [P_2]$ the possible pairs of labels of adjacent vertices are (1,2), (1,3), (1,4), (2,3), (2,4), (3,4). Then obviously $e_f(0) = 1$, $e_f(1) = 5$. That is, $|e_f(0) - e_f(1)| = 4$ and in all other possible arrangement of vertex labels we have $|e_f(0) - e_f(1)| > 4$. Therefore $P_2 [P_2]$ is not a prime cordial graph.

For the graph $P_2 [P_4]$ the possible pairs of labels of adjacent vertices are (1,2), (1,3), (1,4), (1,5), (1,6), (1,7), (1,8) (2,3), (2,4), (2,5), (2,6), (2,7), (2,8), (3,4), (3,5), (3,6), (3,7), (3,8), (4,5), (4,6), (4,7), (4,8), (5,6), (5,7), (5,8), (6,7), (6,8), (7,8) . Then obviously $e_f(0) = 7$, $e_f(1) = 9$. i.e. $|e_f(0) - e_f(1)| = 2$ and in all other possible arrangement of vertex labels we have $|e_f(0) - e_f(1)| > 2$. Thus $P_2 [P_4]$ is not a prime cordial graph.

*Case 2: m even, m ≥ 6*

$f(u_1, v_1) = 2, f(u_2, v_1) = 8,$

$f(u_{2+i}, v_1) = 4i + 10, \quad 1 \leq i \leq m/2 - 3$

$f(u_{m/2}, v_1) = 12,$

$f(u_{m/2+i}, v_1) = 4i - 3, \quad , \quad 1 \leq i \leq m/2$

$f(u_1, v_2) = 4, f(u_2, v_2) = 10,$

$f(u_{2+i}, v_2) = 4i + 12, \quad 1 \leq i \leq m/2 - 3$

$f(u_{m/2}, v_2) = 6, f(u_{m/2+1}, v_2) = 3,$

$f(u_{m/2+1+i}, v_2) = 4i + 3, \quad 1 \leq i \leq m/2 - 1$

Using above pattern we have

$e_f(0) = e_f(1) = \frac{5n-4}{2}$

*Case 3: m = 3*

For the graph $P_2[P_3]$ the possible pairs of labels of adjacent vertices are (1,2), (1,3), (1,4), (1,5), (1,6), (2,3), (2,4), (2,5), (2,6), (3,4), (3,5), (3,6), (4,5), (4,6), (5,6). Then obviously $e_f(0) = 4$, $e_f(1) = 7$. That is, $|e_f(0) - e_f(1)| = 3$ and in all other possible arrangement of vertex labels we have $|e_f(0) - e_f(1)| > 3$. Thus $P_2[P_3]$ is not a prime cordial graph.

*Case 4: m odd, m ≥ 5*

$f(u_i, v_1) = 4(1+i), \quad 1 \leq i \leq \lfloor n/2 \rfloor - 1$

$f(u_{\lfloor n/2 \rfloor}, v_1) = 2,$

$f(u_{\lfloor n/2 \rfloor+1}, v_1) = 6, \quad f(u_{\lfloor n/2 \rfloor+2}, v_1) = 9, \quad f(u_{\lfloor n/2 \rfloor+3}, v_1) = 5,$

$f(u_{\lfloor n/2 \rfloor+2+i}, v_1) = 4i + 7, \quad 1 \leq i \leq \lfloor n/2 \rfloor - 2$

$f(u_1, v_2) = 4,$

$f(u_{1+i}, v_2) = 4i + 6, \quad 1 \leq i \leq \lfloor n/2 \rfloor - 1$

$f(u_{\lfloor n/2 \rfloor+1}, v_2) = 3, \quad f(u_{\lfloor n/2 \rfloor+2}, v_2) = 1, \quad f(u_{\lfloor n/2 \rfloor+3}, v_2) = 7,$

$f(u_{\lfloor n/2 \rfloor+2+i}, v_2) = 4i + 9, \quad 1 \leq i \leq \lfloor n/2 \rfloor - 2$

Using above pattern we have

$e_f(0) = e_f(1) + 1 = 2n + \lfloor n/2 \rfloor - 1.$

Thus in case 2 and case 4 the graph $P_2[P_m]$ satisfies the condition $|e_f(0) - e_f(1)| \leq 1$.

That is, $P_2[P_m]$ is a prime cordial graph $\forall\, m \geq 5$.

*Illustration 2.6* Consider the graph $P_2[P_5]$. The prime cordial labeling is as shown in *Fig 5*.

*Theorem 2.7 Two* cycles joined by a path $P_m$ is a prime cordial graph.

*Proof*: Let $G$ be the graph obtained by joining two cycles $C_n$ and $C'_n$ by a path $P_m$. Let $v_1, v_2, v_3, \ldots\ldots v_n, v'_1, v'_2, v'_3 \ldots\ldots v'_n$ be the vertices of $C_n$, $C'_n$ respectively. Here $u_1, u_2, u_3, \ldots\ldots$ are the vertices of $P_m$. We define vertex labeling $f: V(G) \rightarrow \{1, 2, 3, \ldots\ldots |V(G)|\}$ as follows. We consider following four cases.

*Case 1: m odd, m ≥ 5*

$f(u_1) = f(v_1) = 2, f(v_2) = 4,$

$f(v_{i+2}) = 2(i+3), \quad 1 \leq i \leq n - 2$

$f(u_{i+1}) = f(v_n) + 2i, \quad 1 \leq i \leq \lfloor m/2 \rfloor - 2$

$f(u_{\lfloor m/2 \rfloor}) = 6, \quad f(u_{\lfloor m/2 \rfloor+1}) = 3, \quad f(u_{\lfloor m/2 \rfloor+2}) = 1$

$f(u_{\lfloor m/2 \rfloor+2+i}) = 2i + 3, \quad 1 \leq i \leq \lfloor m/2 \rfloor - 1$

$f(v'_1) = f(u_m), \quad f(v'_{i+1}) = f(v'_1) + 2i, \quad 1 \leq i \leq n - 1$

In view of the above defined labeling pattern we have

$e_f(0) = e_f(1) = n + \lfloor m/2 \rfloor.$

*Case 2: m = 3*

$f(u_1) = f(v_1) = 6, f(v_2) = 2, f(v_3) = 4,$

$f(v_{i+3}) = 2(i+3), \quad 1 \leq i \leq n - 3$

$f(u_2) = 3, f(v'_1) = f(u_3) = 1, \quad f(v'_2) = 5$

$f(v'_{2+i}) = 2i + 5, \quad 1 \leq i \leq n - 2$

In view of the above defined labeling pattern we have

$e_f(0) = e_f(1) = n + 1$

Case 3: m even, $m \geq 4$

$f(u_1) = f(v_1) = 2, f(v_2) = 4,$

$f(v_{i+2}) = 2(i + 3), \quad 1 \leq i \leq n - 2$

$f(u_{i+1}) = f(v_n) + 2i, \quad 1 \leq i \leq m/2 - 2$

$f(u_{m/2}) = 6, \quad f(u_{m/2+1}) = 3, \quad f(u_{m/2+2}) = 1$

$f(u_{m/2+2+i}) = 2i + 3, \quad 1 \leq i \leq m/2 - 2$

$f(v'_1) = f(u_m), \quad f(v'_{i+1}) = f(v'_1) + 2i, \quad 1 \leq i \leq n - 1$

In view of the above defined labeling pattern we have

$e_f(0) = e_f(1) + 1 = n + m/2$

Case 4: $m = 2$

$f(u_1) = f(v_1) = 2$

$f(v_{1+i}) = 2(i + 1), \quad 1 \leq i \leq n - 1$

$f(v'_1) = f(u_2) = 1$

$f(v'_{1+i}) = 2i+1, \ 1 \leq i \leq n - 1$

In view of the above defined labeling pattern we have

$e_f(0) + 1 = e_f(1) = n + 1.$

Thus in all cases graph $G$ satisfies the condition $|e_f(0) - e_f(1)| \leq 1$.

That is $G$ is a prime cordial graph.

*Illustration 2.8* Consider the graph joining to copies of $C_5$ by the path $P_7$. The prime cordial labeling is as shown in *Fig 6.*

*Theorem 2.9* The graph obtained by switching of an arbitrary vertex in cycle $C_n$ admits prime cordial labeling except $n = 5$.

*Proof* : Let $v_1, v_2, \ldots . v_n$ be the successive vertices of $C_n$ and $G_v$ denotes the graph obtained by switching of a vertex $v$. Without loss of generality let the switched vertex be $v_1$ and we initiate the labeling from the switched vertex $v_1$.

To define $f: V(Gv_1) \rightarrow \{1, 2, 3 \ldots |V(G)|\}$ we consider following four cases.

Case 1: $n = 4$

The case when $n=4$ is to be dealt separately. The graph $Gv_1$ and its prime cordial labeling is shown in *Fig* 7.

Case 2: $n$ even, $n \geq 6$

$f(v_1) = 2, f(v_2) = 1, f(v_3) = 4$

$f(v_{3+i}) = 2(i+3), \quad 1 \leq i \leq n/2 - 3$

$f(v_{n/2+1}) = 6, f(v_{n/2+2}) = 3$

$f(v_{n/2+2+i}) = 2i + 3, \ 1 \leq i \leq n/2 - 2$

Using above pattern we have

$e_f(0) = e_f(1) + 1 = n - 2$

Case 3: $n = 5$

For the graph $Gv_1$ the possible pairs of labels of adjacent vertices are (1,2), (1,3), (1,4), (1,5), (2,3), (2,4), (2,5), (3,4), (3,5), (4,5). Then obviously $e_f(0) = 1$, $e_f(1) = 4$. That is, $|e_f(0) - e_f(1)| = 3$ and in all other possible arrangement of vertex labels we have $|e_f(0) - e_f(1)| > 3$. Thus, $Gv_1$ is not a prime cordial graph.

Case 4: $n$ odd, $n \geq 7$

$f(v_1) = 2, f(v_2) = 1, f(v_3) = 4$

$f(v_{3+i}) = 2(i+3), \quad 1 \leq i \leq \lfloor n/2 \rfloor - 3$

$f(v_{\lfloor n/2 \rfloor + 1}) = 6, f(v_{\lfloor n/2 \rfloor + 2}) = 3$

$f(v_{\lfloor n/2 \rfloor + 2 + i}) = 2i + 3,\ 1 \le i \le \lfloor n/2 \rfloor - 1$

Using above pattern we have

$e_f(0) + 1 = e_f(1) = n - 2$

Thus in cases 1, 2 and 4 $f$ satisfies the condition for prime cordial labeling. That is, $Gv_1$ is a prime cordial graph.

*Illustration 2.10* Consider the graph obtained by switching the vertex in $C_7$. The prime cordial labeling is as shown in *Fig 8.*

**3. Concluding Remarks**

It is always interesting to investigate whether any graph or graph families admit a particular type of graph labeling? Here we investigate five results corresponding to prime cordial labeling. Analogous work can be carried out for other graph families and in the context of different graph labeling problems.

**References**

Bloom G. S. and Golomb S. W. (1977). Applications of numbered undirected graphs, *Proc of IEEE*, 65(4), 562-570.

Cahit I. (1987). Cordial Graphs: A weaker version of graceful and harmonious Graphs, *Ars Combinatoria*, 23, 201-207.

Gallian, J. A. (2009). A dynamic survey of graph labeling*, The Electronic Journal of Combinatorics*, 16, #DS 6.

Harary, F. (1972). *Graph Theory*, Massachusetts, Addison Wesley.

Sundaram M., Ponraj R. and Somasundram S. (2005). Prime Cordial Labeling of graphs, *J.Indian Acad. Math.,* 27(2), 373-390.

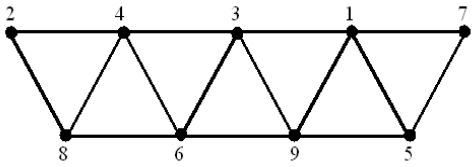


Figure 1. $T(P_5)$ and its prime cordial labeling

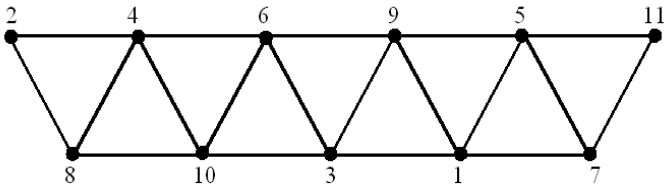


Figure 2. $T(P_6)$ and its prime cordial labeling

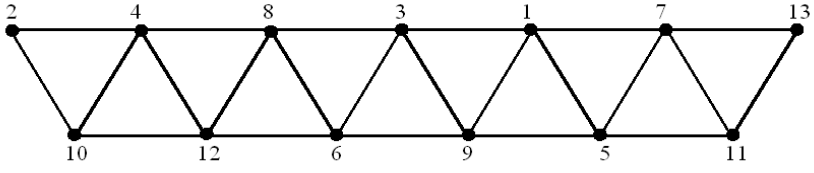


Figure 3. $T(P_7)$ and its prime cordial labeling

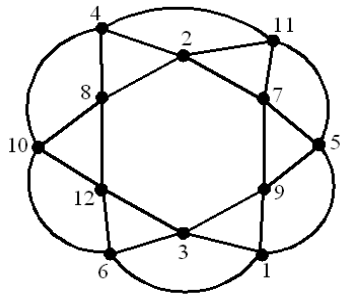


Figure 4. $T(C_6)$ and its prime cordial labeling

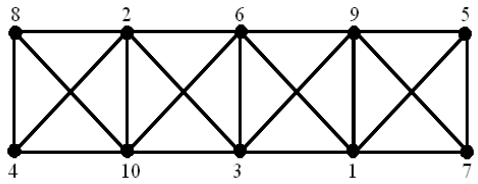


Figure 5. $P_2$ [$P_5$] and its prime cordial labeling

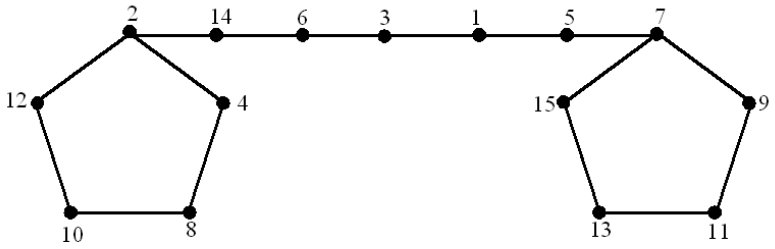


Figure 6. Two cycles $C_5$ join by $P_7$ and its prime cordial labeling

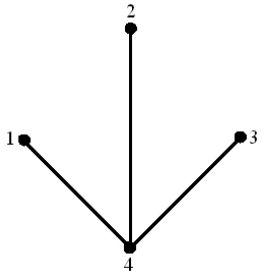


Figure 7. Vertex switching in $C_4$ and its prime cordial labeling

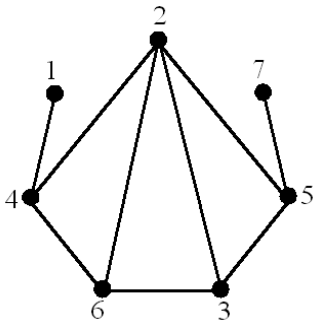


Figure 8. Vertex switching in $C_7$ and its prime cordial labeling


ISSN 1913-1844 E-ISSN 1913-1852

# Deformation Calculating of Electromagnetic Launcher's Rail Subjected to Logarithmic Magnetic Pressure

Wen Liu (Corresponding author) & Min Li
School of Sciences, Yanshan University, Qinhuangdao 066004, China

Xiangzhong Bai
School of Civil Engineering & Mechanics, Yanshan University, Qinhuangdao 066004, China
E-mail: liuwen1961@hotmail.com

Leilei Wang
School of Sciences, Yanshan University, Qinhuangdao 066004, China

*This project is supported by National Natural Science Foundation of China (Grant NO. 50875230).*
*The Excellent Going Abroad Experts' Training Program in Hebei Province.*

**Abstract**

To solve the accurate calculation of force-deformation of the electromagnetic launcher's rail , this is helpful to extend the rail life and improve the firing accuracy. Therefore, the electromagnetic launcher's rail can be modeled as a beam on elastic foundation with simply supported beam by moving load. In this paper Euler beam theory is applied to build the Mechanical model and the analytical solution of the equation subjected to logarithmic magnetic pressure is derived in detail, which has successfully avoided the errors which are caused by using the uniform pressure to approximately replace the variable force. The numerical analysis brings from the elastic coefficient, the damping coefficient, the mass of rail and the load's velocity have influence on the deformation of beam by the MATLAB software. The consequence shows that the elastic coefficient and the load's velocity have quite obvious affect on the deformation of the beam while the damping coefficient and the mass of rail have not obvious affect on the deformation of the beam. It laid the foundation for solve the electromagnetic launcher's rail subjected to magnetic pressure of arbitrary function and promote the practicality of the electromagnetic guns.

**Keywords:** Electromagnetic gun, Launcher's rail, Elastic foundation beam, Damping force, Mechanical model, Lagrange equation

## 1. Introduction

The electromagnetic gun is a new concept weapon, the technology of its has inestimable application potential not only in the military field, but also in aviation, aerospace, transportation, industrial production, scientific research and other fields. Since the 80s, especially in the recent ten years, with the development of new technology and new material, the research of launcher, launching weight, projectile velocity and high efficiency power source in the electromagnetic railgun have reached a series of achievement. The Su Rense.Livermore Nation Laboratory and The Lowes.Alamos Nation Laboratory, once have cooperated to accelerated a projectile weighed 2.2g to a supervelocity of 10km/s. Fluid Physics Institute of the Chinese Engineering Academy had built the first electromagnetic rail launcher, which can accelerate the projectile weighted 0.34g to 16.8km/s. While the velocity of the conventional cannon is only 2km/s, which is so closed to the limitation of physics that the range is not possible to be farther. On the contrary, the thrust of the electromagnetic railgun is ten times bigger than that of the traditional launcher. The projectile can be accelerated to several kilometers or even to dozens of kilometers in one second, for it possesses huge kinetic energy which greatly enhance the range and power of the weapon.

T.Tzeng used the elastic foundation beam to build mechanical model of the electromagnetic railgun and deduced the solve process of governing equation. HU Yuwei analyzed theoretical built model and simulation analysis for the work of the process of electromagnetic railgun. WANG Sheng adopted the Fourier transform to study displacement field due to a moving load on Euler beam resting on an elastic half-space.

However, the damping force to the response of beam is ignored in the above researches. There is no doubt that

the calculation of this kind of situation has the defects of analysis and calculation of mechanical. As a high-tech and high-precision electromagnetic launcher, accurate theoretical analysis and calculation in engineering are require. But until now, no researcher has given any exact analytical solution, thus further analytic solution of the equation subjected to variable pressure is of great significance. In fact, it is of theoretical value to research the theoretical analytic solution of various disciplines, including the analytical solution of practical engineering problems. On the one hand, its mechanical picture can be completely stated, on the other hand it can be used as a standard solution, to widely produce variety of numerical solution.

In this paper, regarding the rail as simply supported beam on the elastic foundation and considering the damping force, a mechanic model which is under the effect of moving load is proposed . Moreover, making use of variable method and the Lagrange equation which considering the damping force, the analytical solution (Liu Wen and San Rui,2009)of the governing equation subjected to nonlinear function pressures is derived and the influences brought from the elastic coefficient, the damping coefficient, the mass of rail and the load's velocity on the response of beam is analyzed.

## 2. Mechanical Model

Fig.1 shows a schematic of an electromagnetic railgun composed of power source, rail, armature and projectile. When the electric current of armature goes through the rail, it forms a strong magnetic field in the area of their encirclement. With the reaction by the magnetic field and the electric current, it emerges powerful electromagnetic force, which pushes the armature and projectile to do the accelerating motion along the rail till the projectile be launched out of the rail.

Fig.2 is the mechanical model of the railgun —simply supported beam partially subjects to nonlinear load in a time-varying region sitting on the elastic foundation. Considering the effect of the beam by the damping force and basing on the Euler beam theory, we obtain the governing equation of elastic foundation beam by moving load which is a transient fourth—order differential equation as follows (S.Timoshenko,1965 and YU Yanli,2002):

$$m\frac{\partial^2 w}{\partial t^2}+EI\frac{\partial^4 w}{\partial x^4}+kw+c\frac{\partial w}{\partial t}=p(x,t) \tag{1}$$

Where $w$ is the deflection, $m=\rho Bh$ is the mass per unit length, $\rho$ is the density of rail material, $B$ and $h$ are respectively the width and thickness of the rail, $EI$ is the bending stiffness of beam, $k$ is the elastic constant, $c$ is the damping coefficient . The function $p(x,t)=q(x)\left[1-H(x-vt)\right]$ in(1), represents the magnetic pressure front traveling along the rail with velocity $v$ represented by a Heaviside step function $H(x-vt)$ ( Jerome T. Tzeng,2005), and $q(x)=q\log_a(x)$ , $a>1$.

## 3. Solution of the Homogeneous Equation

The homogeneous equation is a fourth—order partial differential equation, in order to change it into the ordinary differential equation, we solve it by the method of variable separation.

The solution of the homogeneous equation of (1)can be expressed as follows:

$$w(x,t)=\phi(t)\theta(x) \tag{2}$$

Substituting(2)into the homogeneous equation of(1):

$$m\frac{\partial^2\phi}{\partial t^2}\theta+EI\phi\theta^{(4)}+k\phi\theta+c\theta\frac{\partial\phi}{\partial t}=0 \tag{3}$$

That can be expressed as follows:

$$-\frac{\frac{\partial^2\phi}{\partial t^2}}{c\phi}-\frac{\frac{\partial\phi}{\partial t}}{m\phi}=\frac{EI}{cm}\frac{\theta^{(4)}}{\theta}+\frac{k}{cm} \tag{4}$$

from equation(4), let:

$$-\frac{\frac{\partial^2\phi}{\partial t^2}}{c\phi}-\frac{\frac{\partial\phi}{\partial t}}{m\phi}=\lambda^2 \tag{5}$$

And

$$\frac{EI}{cm}\frac{\theta^{(4)}}{\theta}+\frac{k}{cm}=\lambda^2 \tag{6}$$

That is

$$\theta^{(4)}-\beta^4\theta=0 \tag{7}$$

Where, $\beta^4=\left(\lambda^2-\frac{k}{cm}\right)\frac{cm}{EI}$

solution of equation(5)can be expressed as follows:

$$\phi(t)=Ae^{\frac{-c+R}{2m}t}+Be^{\frac{-c-R}{2m}t} \tag{8}$$

Where, $R^2=c^2-4cm^2\lambda^2>0$

Based on the boundary condition of the simple beam,

$$\begin{cases}\theta(0)=0\\ \left.\dfrac{\partial^2\theta(x)}{\partial x^2}\right|_{x=0}=0\end{cases} \quad \text{and} \quad \begin{cases}\theta(L)=0\\ \left.\dfrac{\partial^2\theta(x)}{\partial x^2}\right|_{x=L}=0\end{cases}$$

solution of equation(7)can be expressed as follows( ZHU Shijian,2006):

$$\theta_i(x)=\sqrt{\frac{2}{mL}}\sin\frac{n\pi}{L}x$$

Accordingly:

$$w_i(x,t)=\theta_i(x)\phi_i(t)=\left(\sqrt{\frac{2}{mL}}\sin\frac{n\pi}{L}x\right)\times\left[A_ie^{\frac{-c+R}{2m}t}+B_ie^{\frac{-c-R}{2m}t}\right]$$

In terms of the orthogonality of $\theta_i(x)$ (ZHANG Xiangting,2006), we obtain:

$$\int_0^L\theta_i\theta_j dx=\begin{cases}0, & \text{at } i\neq j\\ 1, & \text{at } i=j\end{cases}$$

Hence, deformation $w(x,t)$ of the beam can be expressed by the linear combination of $\theta_i(x)$.

$$w(x,t)=\sum_i\theta_i(x)\phi_i(t)=\sum_i\left(\sqrt{\frac{2}{mL}}\sin\frac{n\pi}{L}x\right)\times\left[A_ie^{\frac{-c+R}{2m}t}+B_ie^{\frac{-c-R}{2m}t}\right]$$

Where constants $A_i, B_i$ are determined by the initial conditions.

**4. Analytical Solution of Governing Equation**

The analytical solution of (1) can be obtained by the Lagrange equation including the damping force. Where $T$ is the kinetic energy of the beam, $U$ is the total stain energy, $G$ is the dissipation function(ZHANG Xiangting,2002).

$$\frac{d}{dt}\left(\frac{\partial T}{\partial\dot{\phi}_i}\right)-\frac{\partial T}{\partial\phi_i}+\frac{\partial U}{\partial\phi_i}-\frac{\partial G}{\partial\dot{\phi}_i}=Q_i$$

The kinetic energy of the beam $T$ can be expressed as follows (LOU Ping,2003):

$$T=\frac{1}{2}\sum_i M_i\left(\frac{\partial\phi_i}{\partial t}\right)^2$$

Where $M_i=\int_0^L m\theta_i^2(x)dx$ represents the general mass of the beam.

The total strain energy of the beam $U$ is consisted by the strain energy $U_b$ of the beam, and the strain energy $U_f$ of

the foundation.

$$U_b = \frac{1}{2}\int_0^L EI\left(\frac{\partial^2 w(x,t)}{\partial x^2}\right)^2 dx = \frac{1}{2}\sum_i\sum_j \phi_i\phi_j \int_0^L EI\frac{\partial^2\theta_i}{\partial x^2}\frac{\partial^2\theta_j}{\partial x^2}dx = \frac{1}{2}\frac{EI}{m}\sum_i \beta_i^4 M_i\phi_i^2$$

$$U_f = \frac{1}{2}\int_0^L kw^2 dx = \frac{k}{2}\int_0^L\left(\sum_i \theta_i\varphi_i\right)^2 dx = \frac{k}{2}\sum_i\sum_j \phi_i\phi_j\int_0^L \theta_i\theta_j dx = \frac{k}{2m}M_i\sum_i\phi_i^2$$

The total strain energy $U$ is obtained as:

$$U = U_b + U_f = \frac{1}{2}\frac{EI}{m}\sum_i \beta_i^4 M_i\phi_i^2 + \frac{k}{2m}M_i\sum_i\phi_i^2 \quad = \frac{1}{2}\left[\sum_i M_i\phi_i^2\left(\frac{EI}{m}\beta_i^4 + \frac{k}{m}\right)\right] \quad = \frac{1}{2}\left[\sum_i cM_i\phi_i^2\lambda_i^2\right]$$

The dissipation function $G$ can be expressed as:

$$G = -\frac{1}{2}\int_0^L c\left(\frac{\partial w}{\partial t}\right)^2 dx \quad = -\frac{1}{2}\sum_i\sum_j \frac{\partial\phi_i}{\partial t}\frac{\partial\phi_j}{\partial t}\int_0^L c\theta_i\theta_j dx = -\frac{c}{2m}\sum_i M_i\left(\frac{\partial\phi_i}{\partial t}\right)^2$$

The virtual work done by the magnetic pressure $p(x,t) = q(x)\left[1 - H(x - vt)\right]$ in a virtual displacement $\delta\varphi_i$ can be expressed as follows:

$$\partial W = \int_0^L p(x,t)\delta w_i dx = \sum_i \partial\phi_i\int_0^L p(x,t)\theta_i(x)dx \ = \sum_i \partial\phi_i Q_i$$

Where we define $Q_i$ as the generalized force

$$Q_i = \int_0^L p(x,t)\theta_i(x)dx = \int_0^{vt} q(x)\theta_i(x)dx = \sqrt{\frac{2}{mL}}\int_0^{vt} q\log_a(x)\sin\frac{n\pi x}{L}dx$$

$$= \frac{q\sqrt{\frac{L}{2m}}}{n\pi\ln(a)}\left[2\ln(vt)\left(1 - \cos\left(\frac{n\pi vt}{L}\right)\right) + C_1 e^t\right]$$

Substituting $T, U, G, Q_i$ into the Lagrange equation including the damping force, we obtain an ordinary differential equation:

$$\frac{\partial^2\phi_i}{\partial t^2} + \frac{c}{m}\frac{\partial\phi}{\partial t} + c\lambda_i^2\phi_i = \frac{Q_i(t)}{M_i} = F(t) \tag{9}$$

Where:

$$F(t) = \int_0^L p(x,t)\theta_i(x)dx = \int_0^{vt} q(x)\theta_i(x)dx \quad = \sqrt{\frac{2}{mL}}\int_0^{vt} q\log_a(x)\sin\frac{n\pi x}{L}dx$$

$$= \frac{q\sqrt{\frac{L}{2m}}}{M_i n\pi\ln(a)}\left[2\ln(vt)\left(1 - \cos\left(\frac{n\pi vt}{L}\right)\right) + C_1 e^t\right]$$

The general solution of equation(9)is:

$$\phi_i(t) = \frac{m}{R}\left(\frac{\partial\phi_i(0)}{\partial t} + \frac{c+R}{2m}\phi_i(0)\right)e^{\frac{-c+R}{2m}t} + \frac{m}{R}\left(-\frac{\partial\phi_i(0)}{\partial t} + \frac{-c+R}{2m}\phi_i(0)\right)e^{\frac{-c-R}{2m}t}$$

$$+ \frac{m}{R}\int_0^t F(\xi)\left(e^{\frac{-c+R}{2m}(t-\xi)} - e^{\frac{-c-R}{2m}(t-\xi)}\right)d\xi$$

So the general solution of(1)can be expressed as follows:

$$w(x,t) = \sum_i \theta_i(x)\phi_i(t) = \sum_i \sqrt{\frac{2}{mL}}\sin\frac{n\pi}{L}x\left\{\frac{m}{R}\left(\frac{\partial\phi_i(0)}{\partial t} + \frac{c+R}{2m}\phi_i(0)\right)e^{\frac{-c+R}{2m}t}\right.$$

$$+ \frac{m}{R}\left(-\frac{\partial\phi_i(0)}{\partial t} + \frac{-c+R}{2m}\phi_i(0)\right)e^{\frac{-c-R}{2m}t} \tag{10}$$

$$\left. + \frac{m}{R}\int_0^t F(\xi)\left(e^{\frac{-c+R}{2m}(t-\xi)} - e^{\frac{-c-R}{2m}(t-\xi)}\right)d\xi\right\}$$

The initial conditions are as:

$$\begin{cases} \phi(0) = 0 \\ \left.\dfrac{\partial\phi(t)}{\partial t}\right|_{t=0} = 0 \end{cases}$$

So

$$\phi_i(t)=\frac{m}{R}\int_0^{v\xi}F(\xi)\left(e^{\frac{-c+R}{2m}(t-\xi)}-e^{\frac{-c-R}{2m}(t-\xi)}\right)d\xi \tag{11}$$

According, substituting the solution of (11) into the equation (10), so we can get the solution $w(x,t)$ of (1). The moment and the shear force of the beam in the rail can be further derived from $w(x,t)$, which provides basis for the overall investigation of the dynamic behavior of the electromagnetic railgun.

**5. Numerical analysis**

Since there are differences among materials of electromagnetic rail launcher, the damping force and the rate of moving load will possibly bring influence to the response of the rail(Jerome T. Tzeng 2005, 41: 246-250.). Thus, it is necessary to consider the elastic coefficient, the damping coefficient, the mass of rail and the load's velocity to compare the response of the rail.

A known Material is modulus of rail material $E=120\text{GPa}$ ,the elastic constant $k=2.532\times10^{10}\text{N/m}^2$ , the density of rail material $\rho=8700\text{kg/m}^3$ , the width of rail $B=3\times10^{-2}\text{m}$ ,the thickness of rail $h=1\times10^{-2}\text{m}$ ,the length of rail $L=2\text{m}$ ,the magnetic load collection degree $\text{q}(x)$=110sinx MPa (JF,2006).

Fig.3 shows the deformation of the beam by the elastic coefficient. Along with the elastic coefficient $(k)$ increasing, the curve of time-deformation is a decreasing trend. Under the calculating conditions given by this paper, for the rail of which $k$ equals to $2.532\times10^{10}\text{N/m}^2$ , the deformation $(w)$ of the beam is $-0.9\times10^{-3}m$ ,when the armature moves to the moment $t=1\times10^{-3}$ . While for the rail of which $k$ equals to $5.064\times10^{10}\text{N/m}^3$ , the deformation $(w)$ of the beam is $-0.2\times10^{-3}m$ at the same moment, we can see that the former is $78\%$ smaller than the latter.

Fig.4 shows the deformation of the beam by the damping coefficient. Along with the damping coefficient $(c)$ increasing, the curve of time-deformation is a slowly decreasing trend.

Fig.5 shows the deformation of the beam by the mass of rail. Compared with copper and aluminum rail, the curve of time-deformation has no significant changes.

Fig.6 shows the deformation of the beam by the load's velocity. Along with the load's velocity $(v)$ increasing, the curve of time-deformation is a increasing trend. Under the calculating conditions given by this paper, for the rail of which $v$ equals to $1000\text{m/s}$ , the deformation $(w)$ of the beam is $1.7\times10^{-3}\text{m}$ when the armature moves to the moment $t=1.6\times10^{-3}\text{s}$ . While for the rail of which $v$ equals to $1200\text{m/s}$ , the deformation $(w)$ of the beam is $3.1\times10^{-3}\text{m}$ at the same moment, we can see that the former is $82\%$ smaller than the latter.

**6. Conclusions**

(1)Taking the rail as a simply support beam on the elastic foundation and considering the damping force,a mechanical model for the electromagnetic railgun is built.

"We don't have general solution to nonlinear problems and some particular solutions are as few as treasures in history."( Zheng Zhemin,1994) In this paper, making use of variable method and the Lagrange equation including the damping force, the general solution of the homogeneous part and the analytical solution of the governing equation subjected to logarithmic pressures is derived which enriched and developed the theory of elastic mechanics with the hope to lay the foundation for solving the difficulty problem of electromagnetic rail subjected to arbitrary distribution function pressures.

(2)The deformation of beam which is influenced by the elastic coefficient, the damping coefficient, the mass of rail and the load's velocity are analyzed by the MATLAB software. When the elastic coefficient is larger, the deformation of beam is smaller; when the load's velocity is larger, the deformation of beam is larger, the damping coefficient and the mass of rail have not obvious affect on the deformation of the beam.

**References**

Anthony J. Johnson1 and Francis C.Moon2. (2006). Elastic Waves and Solid Armature Contact Pressure in Electromagnetic Launchers Transactions on Magnetics 2006.3, 472-475.

HU Yuwei. (2007). Modeling and simulation of electromagnetic rail gun system[D]: [Dissertation for the Master Degree]. Harbin Institute of Technology, 2007.

HU Yuwei. (2007). Modeling and simulation of electromagnetic railgun system[D]: [Dissertation for the Master Degree]. Harbin Institute of Technology, 2007.

Jerome T. Tzeng and Wei Sun. (2007). Dynamic Response of Cantilevered Rail Guns Attributed to Projectile/Gun Interaction –Theory. Transactions on Magnetics, 2007, 43: 207-213.

Jerome T. Tzeng. (2005). Dynamic Response of Electromagntic Railgun Due to Projectile Movement Transactions on Magnetics, 2005, 41: 246-250.

Jerome T. Tzeng. (2005). *Structural Mechanics for Electromagnetic Railguns Transactions on Magnetics,* 2005,1, 246-250.

JIN Shangnian, MA Yongli. (2002). *Theoretical Mechanics*. Higher Education Press, 2002, 211-226.

Liu Wen, San Rui. Mathematic Model and Analytic Solution for Cylinder Subject to Exponential Function. *Chinese Journal of Mechanical Engineering,* 2009,22(4) : 587-593.

Liu Wen. Mathematic Model and Analytic Solution for Cylinder Subject to Uneven Pressures. *Chinese Journal of Mechanical Engineering* , 2006,19(4) 574-578.

LOU Ping,ZENG Qingyuan. (2003). Finite element analysis of infinitely long beam resting on continuous viscoelastic foundation subjected to moving loads. *Journal of Traffic and Tran sportation Engineering* 2003, 3: 1-6.

S.Timoshenko. (1965). *Mechanics of material*. Science press 1965,1-15.

Wang sheng. (2007). Displacement field due to a moving load on Euler beam resting on an elastic half-space [D]: [Dissertation for the Master Degree]. Harbin Institute of Technology, 2007.

WANG Ying, XIAO Feng. (1994). *Principle of electricgun.* National Defense Industry Press, 1994. 5-16.

YU Yanli. (2002). The research of the dynamic response of the rail system and viaduct by moving load [D]: [Dissertation for the Master Degree]. Wuhan University of Technology, 2002.

ZHANG Xiangting, WANG Zhipei. (2006). *Structure Vibration Mechanics.* TongJi Univesity Press 2006, 93-117.

Zheng Zhemin. ZhengZheMin corpus. (1994). Beijing: science press, 1994. P286http://www.sj00.com/soft/1481.htm

ZHU Shijian, LOU lingjun. (2006). *Vibration Theory and Vibration Isolation.* National Defense Industry Press 2006,36-66.

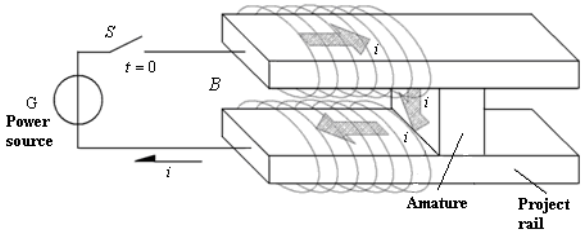


Figure 1. The general diagram of the railgun

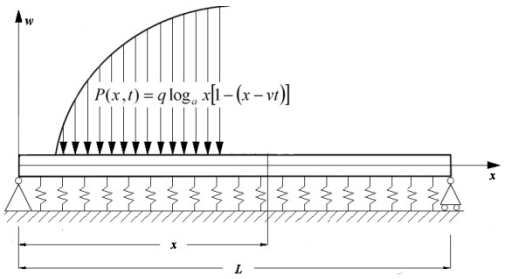


Figure 2. The rail is modeled as a beam on elastic foundation

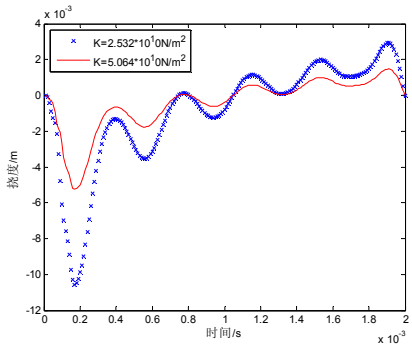


Figure 3. Deformation curve by differences elastic coefficient

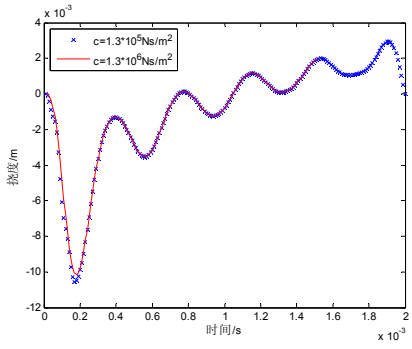


Figure 4. Deformation curve by differences damping coefficient

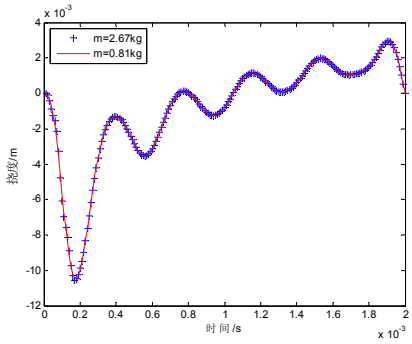


Figure 5. Deformation curve by differences mass of rail

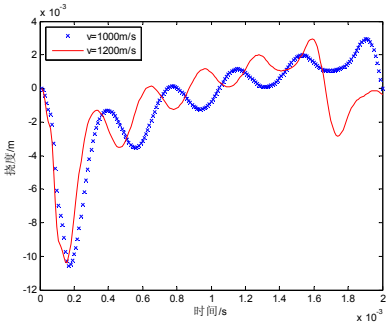


Figure 6. Deformation curve by differences velocity of the load

# Feature Selection Algorithm Using Fuzzy Rough Sets for Predicting Cervical Cancer Risks

Ms. J. Vandar Kuzhali (Corresponding author)
Senior Lecturer / Department of MCA & M.Sc.(S.E.), Erode Sengunthar Engineering College
Thudupathi, Erode(Dt), Tamil Nadu, INDIA – 638 057
Tel: 91-42-9423-2701 Fax: 91-42-9423-2705 E-mail: vandarkuzhali@yahoo.com

Dr. G. Rajendran
Professor & Head / Department of Mathemtics, Kongu Engineering College
Perundurai, Erode(Dt), Tamil Nadu, INDIA – 638 052
Tel: 91-42-9422-6645 Fax: 91-4294-220-087 E-mail: rajendranjv@gmail.com

Mr. V. Srinivasan
Senior Lecturer / Department of MCA, Velalar College of Engineering & Technology
Thindal, Erode(Dt), Tamil Nadu – 638 011
Tel: 91-424-227-0571 Fax: 91-424-243-1725 E-mail: newsrini@rediffmail.com

Mr. G. Siva Kumar
Senior Lecturer / Department of CSE, Erode Sengunthar Engineering College
Thudupathi, Erode(Dt), Tamil Nadu, INDIA – 638 057
Tel: 91-4294-232-701 Fax: 91-4294-232-705 E-mail: gsiva_g@yahoo.com

**Abstract**

Early detection or prediction is very important to reduce the fatalities of Cervical Cancer. Cancer cells affect the Cervix area initially, and then it will spread near by parts. A method using Fuzzy Rough sets is used to analyze the demographic dataset and identify the risk of Cervical Cancer. This method integrates Entropy, Information Gain (IG) and Fuzzy Rough sets for identifying the risk of Cervical Cancer earlier. Risk Factors are identified by IG. Rules are extracted by Fuzzy Rough sets. These rules can be used to identify the risk of Cervical Cancer efficiently than the decision trees. It is found that Human Papilloma Virus (HPV) and having Multiple Sexual Partners (MP) are the major risk factors increase the chances of affecting this cancer. If all the above factors are high the risk of affecting Cervical Cancer is high. Result of this paper will help to improve the clinical practice guidance for analyzing the risk of Cervical Cancer.

**Keywords:** Cervical cancer, Entropy, Information gain, Fuzzy rough sets, Demographic data, Feature selection

## 1. Introduction

Cervical Cancer is the commonest cancer in Indian Women and occupies the top rank among cancers in women. In most developing countries Cervical Cancer constitutes 34% of all women cancers. In India the incidence of this cancer in females is 100 000 / year. It is the 1/5 of the world cancer occurrence among women (Report of WHO consultation, 2009). HPV is the main factor that spreads and causes Cervical Cancer through sexual intercourse (Muñoz N et al, 2002 ; Kahn J. A et al, 2007). The co-factors are Multiple Sexual partners, Very younger age at first sexual act, Husband's extra family affairs, Low socio-Economic factors, Parity & Prolong use of Oral Contraceptive pills.

The American Cancer Society confirmed that the risk of occurring cervical cancer is low in women who have never experience in sexual intercourse. Waiting to have sex until the women is older can help to avoid HPV. It also helps to limit the number of sexual partners and to avoid having sex with someone who has had many other sexual partners. Women those with four full-term pregnancies (Parity) are having the high risk of developing cervical cancer (M. Klitsch, 2002) . There is a potential long term relationship between prolonged use of oral contraceptives and development of Cervical Cancer (Moreno V et al, 2002). Low socio-economic status (SES) is

recognized as a risk factor for many health problems, including cervical cancer, particularly in low-resource settings. Women with low SES often have limited income, restricted access to health care services, poor nutrition, and a low level of awareness about health issues and preventive behavior. All of these factors can make them more vulnerable to illness and preventable diseases such as cervical cancer (Ann L. Coker et al, 2006).

The most common treatments are Hysterectomy, radiation therapy & chemotherapy. Surgery involves removing the uterus and nearby reproductive organs such as the fallopian tubes and ovaries. Lymph nodes near the tumor also may be removed during surgery to see if they contain cancer. After the treatment is finished, most women can lead normal lives. If their uterus was removed, however, they can no longer bear children. This often is not an issue for women in their fifties and sixties, but younger women in their twenties, thirties, and forties may find it hard to adjust to this reality.

The new treatment methods in the field of cancer are introduced everyday. But, the decision making is the complex practice should be done with extreme care and conscious. Sometimes making decisions with intuitive thinking may lead to wrong diagnosis and treatment. Methodological decision making is unfailing and will be the base for the decisions. Instead of identifying the stages and development of cancer, it is important to identify the risk possibility of Cervical Cancer for prevention.

This paper mainly concentrates on identifying the possible risk factors of cervical cancer. This was tested under a group of sample data sets. This is the main aim of this work. In the following sub-divisions the different processes involved in the system are given and the preliminary results were shown with sample data.

## 2. Review of Current Diagnosing Systems

The Pap smear has been the main test for number of years. But, the sensitivity and the specificity are not high. The next highly used technique is Colposcopy. It is the microscopic observation of the Cervix. In this test, Cervix is examined with low and high magnification. Acetic Acid and Lugol solution is applied in the Cervix for differentiating the normal cells and cancerous cells. The visual analysis of Colpscopic image is based on the color variations. This test is mainly used to assess the size, location and the distribution of the lesion. Colposcopy can determine not only the cancer, but also where the tumor is. But Colposcopy requires more experience for the correct analysis of the asymptomatic woman and recognizing the areas of biopsy. This method of test needs long-term experience and more training to get skill in Cancer cell pattern recognition. In these methods of tests clinicians may also add their intuitive decision making than analytical decision making. Additionally the methods for prevention or Early Detection are urgently needed.

In our method pure analytical decision making is done with Entropy and IG as the base, followed with Fuzzy Rough Sets, set of rules are framed. By applying this method one can identify the possible risk of Cervical Cancer from the Demographic factors. The main aim of this method is to prevent the Cervical Cancer.

## 3. Related Work

Decision trees are used to classify the objects. It is a structure that can be used to divide up a large collection of records into successively smaller sets of records by applying a sequence of simple decision rules. A decision tree model consists of a set of rules for dividing a large heterogeneous population into smaller, more homogeneous groups with respect to a particular target variable. These trees are like binary trees. They can be un-even in depth. It is useful to show the proportion of the data in each of the desired classes. Though they are good in many ways, the output must be categorical one. It is also limited to one output attribute. Decision trees are unstable. Trees created from numeric data sets are complex. (Quinlan J. R., 1986)

Here an algorithm named as Feature Selection Algorithm based on Fuzzy Rough Sets predicting Cervical Cancer risk is introduced in this paper. This will filter the irrelevant or noisy attributes from the data set. So, the prediction will be made easily. A major advantage of information theory is its nonparametric nature. Entropy does not require any assumptions about the distribution of variables. Also it does not assume a linear model. It can be applied on categorical time series data. After calculating Entropy and IG, a Fuzzy Rough set analysis is applied instead of Decision Trees for efficiency.

## 4. Methods

### *4.1 Feature Selection*

Feature selection is a technique used to reduce the number of features before applying any algorithms to produce better results. Irrelevant features may have negative effects on a prediction task. Moreover, the computational complexity of a classification algorithm may suffer from the curse of dimensionality caused by several features. When a data set has too many irrelevant or noisy variables and only a few examples, over-fitting is likely to

occur. In addition, data are usually better characterized using fewer variables. Here for feature selection process Entropy and IG are used.

*4.2 Entropy* **:**

It is a measure of variability in a random variable. It is a measure of how pure or impure a variable is.

$$Entropy(S) = \sum - P(I) \log_2 P(I) \quad (1)$$

S- Collection of Samples.

c- Set of outcomes.

P(I) – Proportion of S to the class I.

*4.3 Information Gain***:**

The information gain is based on the decrease in entropy after a dataset is split on an attribute. First the attribute that creates the most homogeneous branches are identified.

$$Gain(S, A) = Entropy(S) - \sum ((|S_y| / |S|) * Entropy(S_y)) \quad \text{(Ross Quinlan, 1993)} \quad (2)$$

*4.4 Fuzzy Rough Set:*

A Rough set is a formal approximation of a Crisp set, in terms of a pair of sets which give lower and upper approximation of the original set. The Lower and Upper approximation sets are crisp sets.

This is the mathematical tool to process the uncertain knowledge. A knowledge representation system is defined as K = (U, A) where, $X \subseteq U$ . U is a non-empty finite set of objects. A is the finite set of primitive attributes. R is an equivalence relation defined on U. U/R indicates the partition of R on U. An ordered pair (U, R) is called the approximation space and any subset is called a concept. Each concept X can be defined as Lower and Upper approximation. (Z. Pawlak, 1982; Z. Pawlak, 1991)

The target set X can be approximated using only the information contained with in P by constructing the P-lower approximations of X.

$$\underline{P}X = \{x / [x]_P \subseteq X\} \quad (3)$$

It is the union of all the equivalence classes in $[x]_P$ which are contained by the target set.

**5. Proposed Method & Experiment**

A sample fuzzified data set is given to show the proposed method. This method is used to extract decision rules to find the risk of Cervical Cancer. Each patient record contains the set of attributes and one decision attribute specifies the risk of Cervical Cancer.

*5.1 Membership Degree*

The membership function of a fuzzy set represents the degree of truth as an extension of valuation. For any set X, a membership function on X is any function from X to the real unit interval [0,1]. It is represented as $\mu_A$. $\tilde{A}$ is the fuzzy set. $\mu_A(x)$ is the membership degree of x in the fuzzy set. $\mu_A(x)$ computes the grade of membership of the element x to the fuzzy set $\tilde{A}$. If x is a member of fuzzy set, then the value is 1, other wise 0. (. L. Zadeh, 1965 ; Goguen J. A. ,1967) This can be defined as

$$\mu_A(x) = \begin{cases} 1, & if \quad x \in A \\ 0, & if \quad x \notin A \end{cases}$$

This is shown in figure I.

*5.2 Fuzzification*

Initially the data set is represented using a function called membership function for mapping the elements according to the degree of membership. Here the quantitative value is transferred to fuzzy sets. Two linguistic

terms used here Y(Yes) & N(No). These two membership values are produced for each attribute according to the membership functions. The sample fuzzified result is shown in Table I. This is done for the calculation efficiency.

*5.3 Feature Selection Algorithm to Predict Cervical Cancer*

1) Find Entropy from the fuzzified dataset.

Entropy (S) =Σ – P(I)$\log_2$ P(I).

2) Calculate IG. Gain(S,A) = Entropy(S) - Σ((|$S_v$|/|S|)* Entropy($S_v$))

3) If Gain (attribute(i)) > Threshold value Select attribute(i) for further processing. Other wise discard it.

4) Find the Equivalence Class. Equiv(i) = Collection of attributes with similar membership values.

5) Generate Discerning Matrix from the Equivalence class. D=a or b or c or avb or avc or bvc or avbvc if Equiv(i) ≠ Equiv(j). D=X(Null) otherwise.

6) Find the Reduct set.

7) Extract Rules for Disease analysis.

Entropy is a mathematical method of study and used here for analyzing the risk of Cervical Cancer. It is used to find the initial result of the total clinical sample data set that is used for further analysis in IG. Entropy is the base used to find the initial result of the total dataset. This Entropy is applied for positive examples and Negative examples in an attribute set. For example 'High' Risk of HPV comes under the group of positive and the 'Low' Risk of HPV is in Negative.

Based on the Entropy results of each attribute or factor, IG is calculated. Each IG is compared with the threshold value. IG values which produce a higher gain than the threshold value are taken as major risk factors of the Cervical Cancer. Entropy and IG values range from 0 to 1. If all factors of the sample data set belong to same class i.e. YES, the value of Entropy is 0.

By considering the resultant major Risk Factors, Equivalence classes were created. Positive region is built by using Lower Approximations. Decision tables are generated for extracting the rules. Instead of making intuitive decisions, this analytical decision making will assist the clinicians efficiently. Intuitive decision making may lead to over treatment for an asymptomatic woman. Using this method, women with the possibility of high risk of Cervical Cancer can be identified, screened and advised for biopsy.

The sample data set after IG calculation is shown in Table II. This is named as Feature Selection. Here, Entropy for the total data set is calculated. Entropy(S) = 0.97104. IG for each attribute is calculated. It is shown in table III. Threshold value is fixed. The factors that are exceeding the threshold value are considered as the Major Risk Factors. It is shown in figure II. These are taken for creating Equivalence classes. It is shown in Table IV.

From the above table discerning matrix is built from the equivalence classes. HPV is assigned as the factor a, MP is assigned as b and Low SES is c. A 5 X 5 matrix is built. Discern = $(D)_{5X5.}$ Here if Equiv-i ≠ Equiv-j then they can be considered in the discerning matrix. The result is shown in Table V. Reduct set of Table V is shown in Table VI. From Table VI rules can be extracted in the IF-THEN format.

From the table VI, the following rules are extracted.

(i) IF HPV Risk = HIGH AND MP>1 THEN Risk of Cervical Cancer=HIGH

(ii) IF HPV Risk = LOW AND MP>1 THEN Risk of Cervical Cancer = HIGH

(iii) IF HPV Risk = HIGH AND MP>1 AND Low SES = YES THEN

Risk of Cervical Cancer = HIGH

(iv) IF HPV Risk = HIGH AND MP=1 THEN Risk of Cervical Cancer = LOW

(v) IF Low SES = Yes THEN Risk of Cervical Cancer = LOW

While using decision trees, they can produce only binary results. More over, they induce the sequential results. Some times class overlap problem may occur. Decision trees are having complex production rules. Also, a decision tree can be sub-optimal. A sample decision tree is given in Figure III.

## 6. Conclusion

In this paper an algorithm is suggested for predicting the risk of Cervical Cancer. Our result shows that the factors HPV, Multiple partners and Low SES are the major factors that will drive to Cervical Cancer. Extracting rules from fuzzy rough sets are producing better results than the decision trees. Studies have reported that the women with a Lower SES are having the risk of affecting Cervical Cancer. Diagnosing Cervical Cancer with the help of symptoms may some times lead to wrong decisions and over treatment. But, this method of detecting the risk of Cervical Cancer will surely be an aid for Clinicians with High Sensitivity and Specificity.

## References

Ann L. Coker, Xianglin L. Du, Shenying Fang and Katherine S. Eggleston. (2006). Socio Economic Status and cervical cancer survival among older women: Findings from the SEER–Medicare linked data cohorts, *Gynecologic Oncology,* Volume 102, Issue 2.

A Report of a WHO consultation. (2009). *about Cervical Cancer in Developing Countries.*

Goguen J. A. (1967). "L-Fuzzy Sets", *Journal of Mathematical Analysis and Applications* 18.

Kahn J. A, Lan D, Kahn R S. (2007). Socio Demographic Factors Associated with High Risk of HPV Infection. *Obstet Gynecol.* 110(1).

L. Zadeh. (1965). *Fuzzy Sets Information and Control,* Vol.3(8).

M. Klitsch. (2002). Long-term pill use, high parity raise cervical cancer risk among women with Human Papilloma Virus infection - Digests - Brief Article, *Perspectives on Sexual and Reproductive Health 6.*

Moreno V, Bosch FX, Muñoz N, et al. (2002). Effect of oral contraceptives on risk of cervical cancer in women with human papillomavirus infection: *the IARC multi -centric case-control study.* Lancet 359(9312).

Muñoz N, Franceschi S, Bosetti C, et al. (2002). Role of parity and human papillomavirus in cervical cancer: *the IARC Multi-centric case-control study.* Lancet 359 (9312).

Quinlan, J. R. (1986). *Induction of Decision Trees.* Mach. Learn. 1.

Ross Quinlan J. (1993). *Machine Learning,* 1st ed. Morgan Kaufmann Publishers Inc.

www.cancer.org American Cancer Society.

Z. Pawlak. (1982). "Rough Sets", *International Journal of Computer and Information Sciences,* Vol.11.

Z. Pawlak. (1991). *Rough Sets - Theoretical Aspect of Reasoning about Data,* Kluwer Academic Pubilishers.

Table 1. Fuzzified Data Set

| Patient No. | Risk of HPV | Multiple Partners (MP) | Young Age at First Sexual Act (AFSA) | Husband's Extra Family Affairs (EFA) | Low Socio Economic Status (Low SES) | Parity ( Minimum of 4 full term pregnancies) | Oral Contraceptive Pills | Risk of Cervical Cancer |
|---|---|---|---|---|---|---|---|---|
| 1 | Y | Y | Y | Y | Y | Y | Y | High |
| 2 | N | Y | Y | N | Y | N | N | High |
| 3 | N | N | Y | Y | Y | N | N | High |
| 4 | Y | Y | N | N | Y | Y | Y | High |
| 5 | Y | N | N | N | Y | Y | N | Low |
| 6 | N | Y | Y | Y | Y | N | N | High |
| 7 | N | N | Y | N | N | Y | Y | Low |
| 8 | N | Y | Y | N | Y | N | N | High |
| 9 | Y | N | N | N | Y | Y | N | Low |
| 10 | N | N | N | N | N | N | N | Low |
| 11 | N | N | Y | N | N | Y | Y | Low |
| 12 | Y | N | N | N | Y | Y | N | Low |
| 13 | N | Y | Y | Y | Y | N | N | High |
| 14 | N | Y | Y | N | Y | N | N | High |
| 15 | N | Y | Y | N | Y | N | N | High |
| 16 | N | N | N | N | N | N | N | Low |
| 17 | Y | N | N | N | Y | Y | N | Low |
| 18 | Y | N | N | N | Y | Y | N | Low |
| 19 | N | Y | Y | Y | Y | N | N | High |
| 20 | N | N | Y | Y | Y | N | N | High |
| 21 | N | N | Y | N | N | Y | Y | Low |
| 22 | Y | Y | Y | Y | Y | Y | Y | High |
| 23 | Y | N | N | N | Y | Y | N | Low |
| 24 | Y | Y | N | N | Y | Y | Y | High |
| 25 | Y | Y | N | N | Y | Y | Y | High |
| 26 | N | Y | Y | N | Y | N | N | High |
| 27 | N | Y | Y | N | Y | N | N | High |
| 28 | N | N | Y | Y | Y | N | N | High |
| 29 | N | N | N | N | N | N | N | Low |
| 30 | Y | Y | Y | Y | Y | Y | Y | High |

Table 2. Feature Selection

| Patient No. | Risk of HPV | Multiple Partners (MP) | Low Socio Economic Status (Low SES) | Risk of Cervical Cancer |
|---|---|---|---|---|
| 1 | Y | Y | Y | High |
| 2 | N | Y | Y | High |
| 3 | N | N | Y | High |
| 4 | Y | Y | Y | High |
| 5 | Y | N | Y | Low |
| 6 | N | Y | Y | High |
| 7 | N | N | N | Low |
| 8 | N | Y | Y | High |
| 9 | Y | N | Y | Low |
| 10 | N | N | N | Low |
| 11 | N | N | N | Low |
| 12 | Y | N | Y | Low |
| 13 | N | Y | Y | High |
| 14 | N | Y | Y | High |
| 15 | N | Y | Y | High |
| 16 | N | N | N | Low |
| 17 | Y | N | Y | Low |
| 18 | Y | N | Y | Low |
| 19 | N | Y | Y | High |
| 20 | N | N | Y | High |
| 21 | N | N | N | Low |
| 22 | Y | Y | Y | High |
| 23 | Y | N | Y | Low |
| 24 | Y | Y | Y | High |
| 25 | Y | Y | Y | High |
| 26 | N | Y | Y | High |
| 27 | N | Y | Y | High |
| 28 | N | N | Y | High |
| 29 | N | N | N | Low |
| 30 | Y | Y | Y | High |


ISSN 1913-1844 E-ISSN 1913-1852

Table 3. Gain Results for Risk Factors

| Risk Factors | Gain |
|---|---|
| HPV | 0.420026 |
| MP | 0.61006 |
| AFSA | 0.256424 |
| EFA | 0.28128 |
| Low SES | 0.32197 |
| Parity | 0.12453 |
| Oral Pills | 0.00721 |

Table 4. Equivalence Class

| | HPV | MP | Low SES | Risk |
|---|---|---|---|---|
| **Equiv – 1** | Y | Y | Y | Y |
| **Equiv – 2** | N | Y | Y | Y |
| **Equiv – 3** | N | N | Y | Y |
| **Equiv – 4** | Y | N | Y | N |
| **Equiv - 5** | N | N | N | N |

Table 5. Discerning Matrix

| | E1 | E2 | E3 | E4 | E5 | R |
|---|---|---|---|---|---|---|
| **E1** | - | a | aVb | b | aVbVc | R1 |
| **E2** | a | - | b | avb | bVc | R2 |
| **E3** | aVb | b | - | a | c | R3 |
| **E4** | b | aVb | a | - | aVc | R4 |
| **E5** | aVbVc | bVc | c | aVc | - | R5 |

Table 6. Reduct Set

| Patient No. | HPV(a) | MP(b) | Low SES(c) | Risk of Cervical Cancer |
|---|---|---|---|---|
| E1 | Y | Y | X | Y |
| E2 | N | Y | X | Y |
| E3 | Y | Y | Y | Y |
| E4 | Y | N | X | N |
| E5 | X | X | N | N |

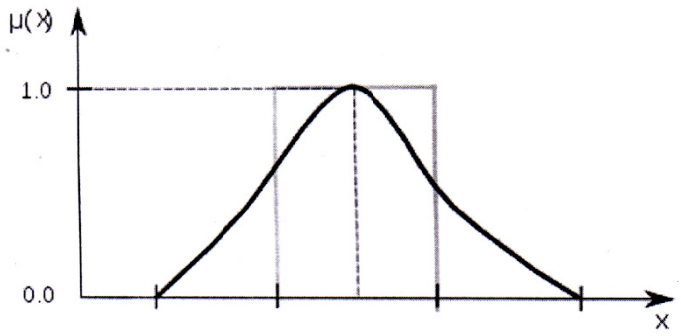


Figure 1. Membership Function

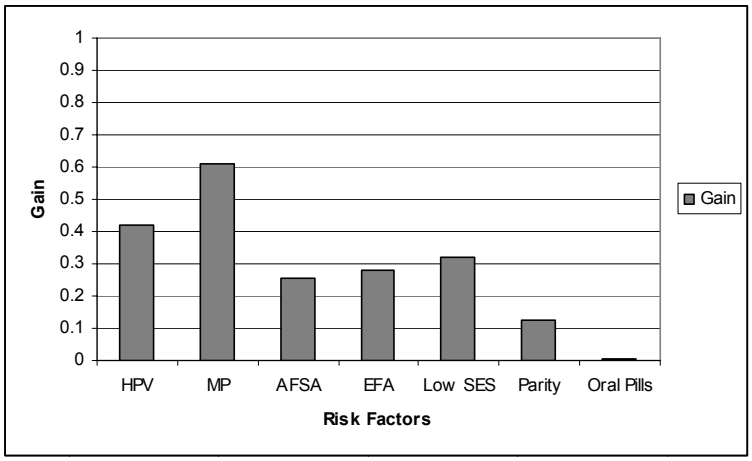


Figure 2. Results of Gain Calculation

 ISSN 1913-1844 E-ISSN 1913-1852

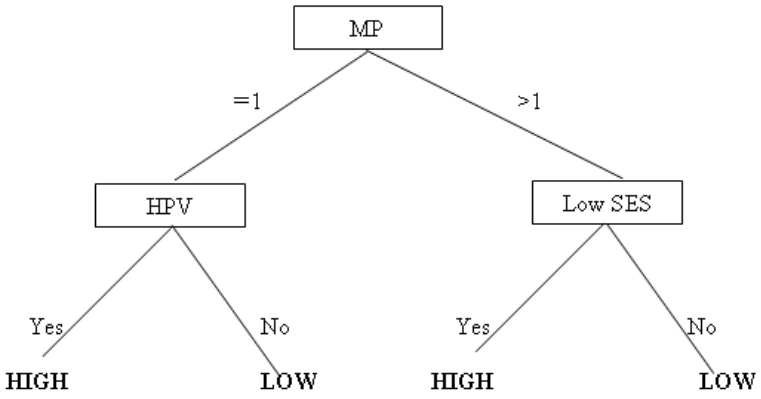


Figure 3. Decision Tree

# Autoregression and Decision Making under Uncertainty

Utkarsh Shrivastava (Corresponding author)
ABV- Indian Institute of Information technology and Management Gwalior
R.No-319, BH-1, AB Road, Gwalior, India-474010
Tel: 91-98-9357-2340 E-mail: utkarsh@students.iiitm.ac.in

Gyan Prakash
ABV- Indian Institute of Information technology and Management Gwalior
R.no- 109, E-block, ABV-IIITM, Gwalior, India-474010
Tel: 91-0751-244-9834 E-mail: gyan@iiitm.ac.in

Joydip Dhar
ABV- Indian Institute of Information technology and Management Gwalior
R.no- 103 E-block, ABV-IIITM, Gwalior, India-474010
Tel:91-0751-2449829, E-mail: jdhar@iiitm.ac.in

Arti Omar
ABV- Indian Institute of Information technology and Management Gwalior
AB Road, Gwalior, India-474010
Tel: 91-92-0220-5934 E-mail: ipg_2008108@students.iiitm.ac.in

**Abstract**

There are innumerable social and economic situations in which we are influenced in our decision making by what others are doing. Under uncertainty it's general tendency of an individual to get inspired by decisions of others or mass opinion. However, such herd behavior many times leads to autoregressive affect i.e. output at some moment is weighted average of past few observation. Hence can autoregressive models be used to predict the outcomes in the situations exhibiting such behavior? Studies have already been done on herd behavior in financial market. So, can models used to forecast financial markets be used to predict general decision making under uncertainty. To prove the validity of the point we conduct a small experiment of human decision making under uncertainty and try to forecast future responses using autoregressive models. A group of students were surveyed such that they can also look upon previous responses which would promote herding. A unique financial market type framework is used to quantify the responses and time series models of auto regression are used to forecast mass opinion.

**Keywords:** Herd mentality, Autoregressive process, Decision making

## 1. Introduction

There are innumerable social and economic situations in which we are influenced in our decision making by what others are doing. Perhaps the common example is from our everyday life we often patronize on what stores and restaurants to patronize and what school to attend based upon their popularity. But it has been suggested by Keynes [1936], for example that this is how investors in asset markets behave. Voters are known to be influenced by opinion polls to vote in the direction that poll predicts to win, this is another instance of going with the flow The same kind of influence is also at work for example academic researchers choose to work on the topic which is currently hot.

In recent years, there has been much interest, both theoretical and empirical, on the extent to which trading in financial markets is characterized by herd behavior. Such an interest stems from the effects that herding may have on financial markets' stability and ability to achieve allocative and informational efficiency. The theoretical literature has tried to identify the mechanisms that lead traders to herd (for surveys, see, e.g., Gale, 1996; Hirshleifer and Teoh, 2003; Chamley, 2004; Vives, 2007). The theoretical contributions have emphasized that, in financial markets, the fact that prices adjust to the order flow makes it more difficult for herding to arise than in

other setups, such as those studied in the social learning literature, where there is no price mechanism. Nevertheless, it is possible that rational traders herd, e.g., because there are different sources of uncertainty in the market. To test herding models directly with data from actual financial markets is difficult. In order to test for herd behavior one needs to detect whether agents choose the same action independently of their private information. The problem for the empiricist is that there are no data on the private information available to the traders. So, it is difficult to determine whether traders make similar decisions because they disregard their own information and imitate or because they are reacting to the same piece of public information, for instance. To overcome this problem, some authors (Cipriani and Guarino, 2005; Drehman et al., 2005) have tested herd behavior in a laboratory financial market. In the laboratory, participants receive private information on the value of a security and observe the decisions of other subjects. Given these two pieces of information, they choose sequentially if they want to sell, to buy or not to trade a security with a market maker. In the laboratory one can observe the private information that subjects have when making their decisions, so it is possible to test models of herding directly.

This study proposes modeling of human decision making in such a way that option available on a certain issue can be visualized as companies and humans would behave as investors and they have to invest on one single company or a single opinion as trading is done in stock markets. Whole system would behave similar to stock market and it is expected that sudden rise in acceptance of a particular alternative would trigger a surge in its acceptance rate as under circumstances of uncertainty employees would consider the option accepted by most others. A real time survey is conducted to acknowledge the accuracy of the proposed visualization. As an empirical analysis, 58 students of MBA class were asked about their preferable employment location in North Central Region of India. They were giving four options which are similar in various contexts. In this scenario students are investors while options for employment are companies to choose from to invest. As other's responses are viewable so this may affect their decision as in financial market. So this paper tries to forecast capitalization of an option lets say New Delhi. Result will tell about percentage of population who want to be employed in New Delhi.

## 2. Previous Research

Herd behavior describes how individuals in a group can act together without planned direction. The term pertains to the behavior of animals in herds, flocks, and schools, and to human conduct during activities such as stock market bubbles and crashes, street demonstrations, sporting events, religious gatherings, episodes of mob violence and even everyday decision making, judgment and opinion forming.

Herd behavior is a term implying alignment to a mode of collective conduct and is expressed as a "similarity in behavior" following the "interactive observation" of actions and payoffs (arising from those actions) among individuals (Hirshleifer and Teoh, 2003). In the stock market context, herding involves the intentional1 sidelining of investors' private information in favor of the observable "consensus" (Bikhchandani and Sharma, 2001) irrespective of fundamentals (Hwang and Salmon, 2004) and the roots of such behavior can be traced to a series of factors be they of psychological or rational nature. From a psychological viewpoint, the impetus underlying imitation has often been assumed to stem from the human nature itself, in the sense that people may tend towards conformity (Hirshleifer, 2001) as a result of their interactive communication. The latter could be explicit (when people are conversing- Shiller, 1995) or tacit (when people observe others' choices).

However, herding could also be driven by more subtle considerations, if its practice is associated with the realization of informational payoffs (Devenow and Welch, 1996) by those imitating the decisions of others. This is the case when one:

a) Possesses no private information,

b) has private information yet is uncertain about it perhaps because it is of low quality,

c) Considers his information-processing abilities to be inadequate or

d) Perceives others as better-informed.

If a large number of investors decide to discard their private signals and free-ride on the informational content of others' actions, this is expected to bear an adverse effect over the public pool of information and may well pave the way towards the development of "informational cascades" (Banerjee, 1992; Bikhchandani , 1992).

A basic tenet of classical economic theory is that investment decisions reflect agents' rationally formed expectations; decisions are made using all available information in an efficient manner. A contrasting view is that investment is also driven by group psychology, which weakens the link between information and market outcomes. In The General Theory, Keynes (1936) expresses skepticism about the ability and inclination of

"long-term investors' to buck market trends to ensure full efficiency. In his view, investors may be reluctant to act according to their own information and beliefs, fearing that their contrarian behavior will damage their reputations as sensible decision-makers.

Thus Keynes suggests that professional managers will follow the herd' if they are concerned about how others will assess their ability to make sound judgements. There are a number of settings in which this kind of herd behavior might have important implications. One example is the stock market, for which the following explanation of the pre-October 1987 bull market is often repeated: The consensus among professional money managers was that price levels were too high--the market was, in their opinion, more likely to go down rather than up. However, few money managers were eager to sell their equity holdings. If the market did continue to go up, they were afraid of being perceived as lone fools for missing out on the ride. On the other hand, in the more likely event of a market decline, there would be comfort in numbers--how bad could they look if everybody else had suffered the same fate?

The same principle can apply to corporate investment, when a number of companies are investing in similar assets. In Selling Money, Gwynne (1986) documents problems of herd behavior in banks' lending policies towards LDC's.

*2.1 Econometric Modeling*

A time series is defined as a set of quantitative observations arranged in chronological order. It is generally assumed that time is a discrete variable. Time series have always been used in the field of econometrics. Tibergen (1939) constructed the first econometric model for the United States and thus started the scientific research programme of empirical econometrics. At that time, however, it was hardly taken into account that chronologically ordered observations might depend on each other. Durbin and Watson (1950/51) developed a test procedure which made it possible to identify first order autocorrelation. Box and Jenkins (1970) introduced univariate models for time series which simply made systematic use of the information included in the observed values of time series. This offered an easy way to predict the future development of this variable. Granger and Newbold (1975) showed that simple forecasts which only considered information given by one single time series often outperformed the forecasts based on large econometric models which sometimes consisted of many hundreds of equations.

Over recent years rigorous treatments of the time series concepts are presented by Fuller (1996) and Hamilton (1994). Applications of these concepts to financial time series are provided by Campbell, Lo, and MacKinlay (1997), Mills (1999), Gourieroux and Jasiak (2001), Tsay (2001), Alexander (2001), and Chan (2002). The problem we are having in this research is of quantifying each observation as the survey is being filled by each student such after each observation a value represents population with that particular option. In this way a time series will be generated and econometric modeling can be done over it to forecast it

*2.2 Auto Regressive Process*

ARIMA (Auto Regressive Integrated Moving Average) processes are mathematical models used for forecasting. In ARIMA terms, a time series is a linear function of past actual values and random shocks, that is:

$$Y_t = f\ (Y_{t-k},\ e_{t-k}) + e_t,\ \text{where}\ k > 0 \qquad (1)$$

The ARIMA approach to forecasting is based on the following ideas:

- The forecasts are based on linear functions of the sample observations.
- The aim is to find the simplest models that provide an adequate description of the observed data. This is sometimes known as the principle of parsimony.

Each ARIMA process has three parts: the autoregressive (or AR) part; the integrated (or I) part; and the moving average (or MA) part. However, this paper concentrates mainly on autoregressive process as model is mainly concerned with dependence of future responses on past little observation. Integrated part refers to number of times a time series is differenced to make it stationary.

Auto-regressive Process ARIMA (1,0,0) is given by :

$$Y_t = \theta + \Phi Y_{t-1} + e_t \qquad (2)$$

The absolute value of $\Phi < 1$, ($-1 < \Phi < 1$) and $e_t$ pure random process with zero mean and variance $\sigma^2$ and $\theta$ is a constant. $Y_t$ is the time series which is being analyzed in our case its New Delhi share first 30 observation. If $\Phi > 1$, the past values of $Y_{t-k}$ and $e_{t-k}$ have greater and greater influence on $Y_t$, it implies the series is non-stationary with an ever increasing mean. If Bound of Stationary does not hold, the series is not autoregressive; it is either

drifting or trending, and first-difference should be used to model the series with stationary. So, NDS time series will have to be first analyzed for the stationarity then only autoregressive models can be applied on it. Autoregressive Process ARIMA (p, 0,0) is:

$$Y_t = \theta + \Phi_1 Y_{t-1} + \Phi_2 Y_{t-2} + \ldots + \Phi_p Y_{t-p} + e_t \quad (3)$$

Many economic and financial time series are well characterized by an ARIMA(1,0,0) process. Leading examples in finance are valuation ratios (dividend price ratio, price-earning ratio etc), real exchange rates, interest rates, and interest rate differentials (spreads).The partial autocorrelation function (PACF) is a useful tool to help identify AR(p) models. The PACF is based on estimating the sequence of AR. The last coefficient of ARIMA (p,0,0) is called partial autocorrelation coefficient, $\Phi_p$ (eq-4) in this case. For an AR(q) all of the first q partial Autocorrelation coefficients are non-zero, and the rest are zero. This will help us to determine value of p for ARIMA (p,d,0) models. Many economic and financial time series exhibit trending behavior or non-stationarity in the mean. Unit root tests can be used to determine if trending data should be first differenced or regressed on deterministic functions of time to render the data stationary. The stationarity tests of Kwiatkowski, Phillips, Schmidt and Shinn (KPSS) (1992) is used to check the stationarity of NDS time series and Phillips-Perron Unit Root Tests (1988) will be used to determine if trending data should be first differenced or regressed on deterministic functions of time to render the data stationary

## 3. Methodology and Concept

The starting point is a sample survey which includes sample of population having major specific characteristics. A questionnaire is designed in such a way that its options cover major decisional alternatives and are close to each other i.e. similar to each other in various aspects to reduce biasing. Options represent a company and students investors, so if a student goes for a particular option means he buys that company's share and its share price will increase. Taking share price analogues to percentage of people those have chosen that option a time series is obtained which varies each time an student fills the questionnaire. After having collected the questionnaire data comes the analysis part. Principle behind this concept is autoregressive nature of time series models which takes into account only few previous observations before forecasting data but not whole past data. Hence, while taking survey it is expected that before making any decision a student would take a look into decisions taken by few others before him which may influence his decision and lead to autoregressive affect in data collected. An individual may be tempted to believe that others are having a secret information which he is not sure about, hence majority are following that particular option. Generally financial time series are non stationary and have unit roots data collected in the survey will be checked for unit roots and stationary

Question asked to students is which job location they will prefer for employment. This question has four options: - (a) Chandigarch (b) Gurgaon (c) New Delhi (d) Noida. As these four locations are very close to each other in Noth Central region (NCR) of India, hence climatic conditions and distance from far location is nearly same. These cities offer equally attractive job opportunities for the individuals an d comprises major part of NCR region of the country, unless a student doesn't live nearby any place or have a bias related to it, is expected to answer the option answered by his most other friends just before him. This would in coordination with our principle.

After collecting the data or choices of students' share of each option is calculated by using this formula

$$NDS\,[n] = \frac{\text{Number of Students opted for New Delh (after n responses)}}{n} \quad (4)$$

n = number of responses and varies from 1-58 as this survey has 58 students

NDS [n] (New Delhi Share) = % of students that have opted for New Delhi after n students have filled the responses from the sample.

As our sample size is 58 a time series with 58 observations will be obtained. First 30 observations will be used to train model parameters while forecast for next 28 observations will be made. This series is expected to behave similar to price of a stock in stock market and show characteristics similar to financial time series, tests will confirm this test later. Further statistical test will confirm about its stationarity and unit root characteristics. Similarly for options b,c and d their share will be calculated. Initially, all options are given 1 value each as base, so at $0^{th}$ count share of each option is .25 or 25%. Now suppose as first student fills the questionnaire and opts for New Delhi then resulting share figures would be .4 ( 2/5 ) for New Delhi and .2 for remaining options. Similarly, with each student filling the questionnaire this share would change. After getting this questionnaire filled by 58 student's four time series with 58 rows each containing share value changes of respective option is obtained. These series will be analyzed in the same way as a financial time series is analyzed.

## 4. Observation Analysis

As New Delhi has been opted by most of the students until 30 observations, so we will try to forecast next 28 observations and check of its series follows some autoregressive process. Consider New Delhi share (NDS) over 30 entries (Fig (1), below). ACF (Fig (2)) and PAF (Fig (3)) of NDS for first 30 responses is very high and decays slowly which indicates presence of some trend, so NDS will have to be differenced. NDS' and NDS'' represents first and second differenced series. KPSS and Philips Perron test (Table 1 and 2 below) confirms that NDS has unit roots and is non stationary while NDS' and NDS'' are stationary as well as doesn't have unit roots. Fig (4) and Fig (5) shows that PAF becomes zero after 2nd and 3ed lag for NDS' and NDS'' respectively. Hence, it can be said that NDS' and NDS'' follows AR (2) and AR (3) processes and are first and second differenced series of NDS. Finally, Fig (6) and Fig (7) compares next 28 observed and forecasted values of NDS using ARIMA(2,1,0) and ARIMA(3,2,0). According to forecast 52% of total students will finally opt for New Delhi while the observed results show that 49% have gone for Delhi.

## Conclusion

Analysis shows that variations in percentage of population going for a particular option follow similar behavior as a financial time series. Options presented for decision making were kept as unbiased as possible still some biasing may arise due some personal preferences of population; still forecast results are highly motivating under given environment. Results of KPSS and Philips Perron test confirms that time series generated has trending behavior and non-stationary of mean as any other financial time series. ARIMA (3,2,0) forecast greatly follows the trend observed in students responses. Final results differ only by 3%. Autoregressive models to some extent have successfully forecasted group decision making under uncertainty.

## Acknowledgement

Authors are indebted to ABV-IIITM Gwalior for providing necessary infrastructure and support for carrying out this work.

## References

Alexander, C. (2001). *Market Models: A Guide to Financial Data Analysis,* John Wiley & Sons, Chichester, UK.

Baille, R.T. and T. Bollerslev. (1994). The Long Memory of the Forward Premium, *Journal of International Money and Finance*, 13, pp. 555-571.

Banerjee, A.V. (1992). A Simple Model of Herd Behavior, *Quarterly Journal of Economics*, 110, 3, pp. 797-817.

Bikhchandani, S., Hirshleifer, D., and Welch, I. (1992). A theory of fads, fashion, custom, and cultural change as informational cascades, *Journal of Political Economy,* 100, 5, pp. 992-1026.

Bikhchandani, S. and Sharma, S. (2001). Herd Behaviour in Financial Markets, *IMF Staff Papers*, Vol. 47, No3

Blanchard and Diamond. (1990). The Beveridge Curve, *NBER,* Working Paper No. R1405.

Box, G.E.P., and G.M. Jenkins. (1970). Time Series Analysis: Forecasting and Control, *Holden-Day*, San Francisco,

Caballero and Hammour. (1994). The Cleansing Effect of Recessions, *American Economic Review*, American Economic Association, 84,5, pp. 1350-68

Campbell, J.Y., A.W. Lo, A.C., MacKinlay. (1997). The Econometrics of Financial Markets, *Princeton University Press*, Princeton, NJ.

Chamley, Christophe. (2004). *Rational Herds*. Cambridge University Press, Cambridge.

Chan, N.H. (2002). *Time Series: Applications to Finance*, John Wiley & Sons, New York.

Cipriani, Marco and Antonio Guarino. (2005). Herd Behavior in a Laboratory Financial Market, *American Economic Review*, 95(5), pp. 1427-1443.

Clive W.J. Granger and Paul Newbold. (1975). Economic Forecasting: The Atheist's Viewpoint, *Modeling the Economy*, Heinemann, London, pp. 131 – 148.

Devenow, Andrea and Ivo, Welch. (1996). Rational Herding in Financial Economics, *European Economic Review*, 40, pp. 603-615

Donald Cochrane and Guy H. Orcutt. (1949). Application of Least Squares Regression to Relationships Containing Auto correlated Error Terms, *Journal of the American Statistical Association* 44, pp. 32-61.